ELSEVIER

Marine Micropaleontology 36 (1999) 31–63

MARINE MICROPALEONTOLOGY

A size analysis of planktic foraminifera from the Arabian Sea

Frank Peeters [a,*], Ekaterina Ivanova [a], Sandrine Conan [a], Geert-Jan Brummer [b], Gerald Ganssen [a], Simon Troelstra [a], Jan van Hinte [a]

[a] *Free University, Centre of Marine Earth Sciences (CMA, NSG), De Boelelaan 1085, 1081 HV Amsterdam, Netherlands*
[b] *Netherlands Institute for Sea Research, PO box 59, 1790 AB Den Burg, Netherlands*

Received 3 April 1998; accepted 14 September 1998

Abstract

Planktic foraminiferal faunas from different environments in the Arabian Sea were size fractionated using 14 sieves with meshes between 100 and 710 μm, to assess the effect of the sieve mesh size cut off level on the faunal composition and to determine the size frequency distribution of individual species. Nine samples from a plankton pump and a towed net, a sediment trap, a box-core and a piston core were selected, to cover living and settling flux faunas as well as fossil faunas from the sediment. In living faunas, most species show an exponential size frequency distribution, with highest numbers in the finest interval of the size spectrum. In sediment trap and core samples, individual species size frequency distributions may consist of: (1) an exponential distribution of relatively small pre-adult specimens; (2) a Gaussian-shaped distribution of larger specimens, which may be classified as adult or terminal; or (3) a combination of both. The distributions are separated using a best fit technique. The composition of the total planktic foraminiferal fauna strongly changes along the size spectrum. Dominant taxa in >355 μm fractions are *Orbulina universa, Globorotalia menardii, Globorotalia tumida, Globigerinella siphonifera* and *Globigerinoides sacculifer*, in 125–355 μm fractions *Globigerina bulloides, Globigerinoides ruber, Neogloboquadrina dutertrei* and *Globigerinita glutinata*, and in <125 μm fractions *Dentigloborotalia anfracta, Tenuitella compressa, Tenuitella iota, Turborotalita quinqueloba* and the immature specimens of larger species. Consequently, the choice of the sieve mesh size strongly determines the percent composition of the assemblage and in turn the paleoceanographic interpretations based on these counts. Species richness and the Shannon diversity increase with decreasing sieve mesh size, while equitability generally decreases with decreasing size. In the water column approximately 60% of the fauna (>100 μm) is present in the 100–125 μm fraction and 1–6% is larger than 250 μm. In samples representing a settling flux (sediment trap and sediment samples) 29–57% of the fauna is present in the 100–125 μm fraction, while 6–23% is larger than 250 μm. Size frequency distributions of the dextral *Neogloboquadrina* complex (= *Neogloboquadrina dutertrei* and *Neogloboquadrina pachyderma* + P–D intergrades) show a bimodal pattern; a smaller peak reflecting dextral *Neogloboquadrina pachyderma*, and a larger peak of adult *Neogloboquadrina dutertrei*. By applying a best fit technique to the data, the two species may be separated from each other. In size fractions larger than 150 μm most species have reached the adult stage of ontogeny and we recommend this mesh size for standard faunal analysis. In addition, sieve mesh sizes of 125 and 250 μm have to be used to obtain a reliable estimate of the abundance of small and large species, respectively.

Keywords: planktic foraminifera; test size; size frequency distribution; sieve mesh size

* Corresponding author.

0377-8398/99/$ – see front matter
PII: S0377-8398(98)00026-7

1. Introduction

1.1. Objectives and previous work

Planktic foraminifera have been used extensively to trace the extent of past upwelling: their variations in test size, weight, accumulation rate, coiling directions and stable isotopic signature, have been used to reconstruct past and present day oceanographic conditions in the Arabian Sea (e.g. Bé and Hutson, 1977; Kroon and Ganssen, 1989; Ganssen and Kroon, 1991; Caulet et al., 1992; Curry et al., 1992; Steens et al., 1992; Anderson and Prell, 1993; Vergnaud-Grazzini et al., 1995; Naidu and Malmgren, 1995, 1996a,b; Reichart, 1997).

To extract the foraminifera from the sample matrix, sieves with different mesh sizes are used to separate large specimens from the smaller, which are often more difficult to identify. Consequently, a part of the foraminiferal fauna is not included in the analyses. Because relative abundance and species composition change as a function of sieve mesh size (Berger, 1971; Bé and Hutson, 1977; Brummer and Kroon, 1988), different mesh sizes will yield a different faunal composition. Statistical techniques, which rely on foraminiferal counts to reconstruct paleoceanographic/climatic conditions or sea-surface temperature (e.g. Imbrie and Kipp, 1971; Kipp, 1976; CLIMAP, 1981, 1984; Curry and Matthews, 1981; Curry et al., 1992; Giraudeau and Rogers, 1994; Pflaumann et al., 1996), are affected by the micropaleontologist's choice of sieve mesh size. Past and ongoing large research programs have evaded this problem by defining their own standard mesh size for fauna analysis, e.g. 150 μm for sediments (CLIMAP, 1981, 1984), or 202 and 150 μm for zooplankton nets (SCOR, 1990). However, many different mesh sizes have been used in other studies. For instance, Hecht (1976) used >250 μm for core-top samples; Curry et al. (1992) used 63, 125, 150, 250 and 500 μm mesh sizes for sediment trap samples, to study foraminifera in separate fractions; Guptha et al. (1994) used a 200 μm mesh plankton net and subsequently washed residues over a 63 μm sieve; Naidu and Malmgren (1995) used >150 μm for sediment samples; Vergnaud-Grazzini et al. (1995) and Vénec-Peyré et al. (1995) used >125 μm for sediment samples; during NIOP cruises (Van Hinte et al., 1995) 85 and 100 μm nets were used, and many other mesh sizes can be found in literature. This practice obstructs a straightforward comparison of foraminiferal counts. Relative abundance of species is merely one aspect which is size dependent; coiling ratios, average test size calculations, test morphology or isotopic signature of individual species also depend on size, or are otherwise affected by the sieve mesh size which is used (Berger, 1971; Vella, 1974; Hecht, 1976; Brummer and Kroon, 1988; Kroon and Darling, 1995).

The aim of this paper is to investigate how the species composition and number of shells change as a function of sieve mesh size and to determine to what extent size frequency distributions (SFDs) of individual species vary between different environments. The samples selected for this size study are taken from different environments, using different sampling gear. The time represented by each of the samples varies from days, i.e. living populations from the water column, to hundreds of years in case of sediment samples. It is therefore difficult, if not impossible, to relate the differences in the SFDs to e.g. a population's response to upwelling. Our central aim is to illustrate and document test size variability and to study the effect of the sieve mesh size on the faunal composition, rather than identifying the environmental/biological controls which might have caused the differences in size.

Foraminiferal faunas usually contain a number of species. As each species has its own size frequency distribution (Brummer and Kroon, 1988), the changes in the fauna composition as a function of size are the combined result of a changing species composition and the size frequency distribution of the constituent species. In order to convert between data sets based on different mesh sizes, it is necessary to know the SFDs and their variability for individual species.

In the Arabian Sea area a few species have widespread distribution patterns and often dominate in planktic foraminiferal assemblages. In this paper we will focus on these species and discuss their SFDs: *Globigerina bulloides* d'Orbigny, *Globigerinita glutinata* (Egger), *Globigerinoides ruber* (d'Orbigny), *Globigerinoides sacculifer* (Brady), *Neogloboquadrina dutertrei* (d'Orbigny) and dextral *Neogloboquadrina pachyderma* (Ehrenberg). Among

these, *G. bulloides* is the most abundant species in the Arabian Sea upwelling areas and is commonly used as a proxy for upwelling in paleoceanographic studies (Curry et al., 1992; Prell et al., 1992; Anderson and Prell, 1993; Naidu and Malmgren, 1995; Conan and Brummer, 1999).

1.2. Arabian Sea oceanographic setting

Past and present coastal upwelling off Oman/Yemen and Somalia is driven by the monsoon system (e.g. Pickard, 1979; Prell and Kutzbach, 1992; Prell et al., 1992). NIOP station 905 is located off Somalia (Fig. 1), directly below the Great Whirl system (Swallow and Bruce, 1966; Bruce, 1979; Bruce et al., 1980; Schott et al., 1990; Fisher et al., 1996). This region is characterized by strong surface currents and, during the southwest summer monsoon, several clockwise rotating eddies transport relatively low saline waters from the equator northward. In the upper part of the water column, transport is characterized by Ekman flow, resulting in highly variable surface water conditions. Mixing of surface- and upwelled water, in particular at gyre edges, leads to enhanced biological production and maxima of chlorophyll *a* are found during the height of the southwest monsoon (Banse, 1987). The increase of biological productivity is also reflected in the fluxes of *G. bulloides*: high fluxes of this species in sediment traps and *G. bulloides* rich assemblages in the sediment are associated with these upwelled waters and can successfully be used as a proxy for upwelling strength (Prell and Curry, 1981; Cullen and Prell, 1984; Prell and Van Campo, 1986; Clemens et

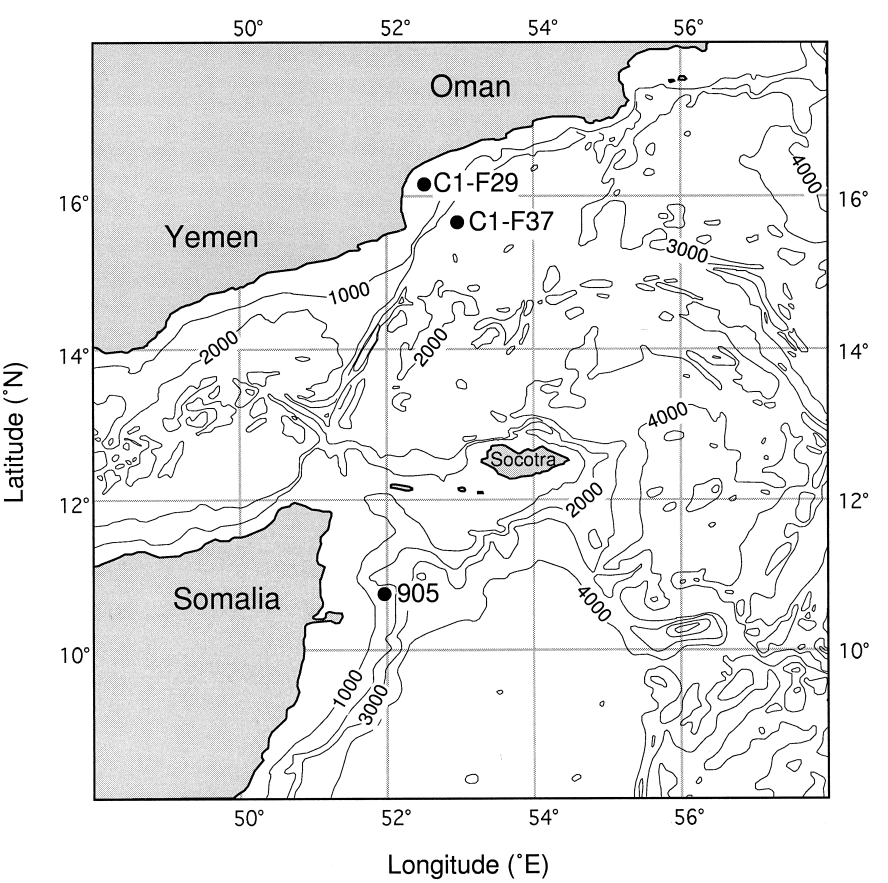

Fig. 1. Map of the southwestern Arabian Sea with the location of NIOP site 905, where plankton net, sediment trap and core samples were collected. The 2 plankton pump samples were collected at stations *C1-F29* and *C1-F37* off Oman/Yemen. Isobaths in meters.

al., 1991; Prell et al., 1992; Naidu and Malmgren, 1996a,b; Conan and Brummer, 1998).

2. Material

This study is part of the multidisciplinary Netherlands Indian Ocean Programme (NIOP), where the geologic component aims to reconstruct the variability of the monsoonal system (Van Hinte et al., 1995). For this purpose an extensive foraminiferal data set from both modern and past environments was collected during NIOP cruises B0/C0, C1 and C2 of R/V *Tyro* in 1992–1993 (Van Hinte et al., 1995). It represents a vertical section from the ocean's surface water to the downcore sediment. The samples were acquired by different techniques i.e. plankton pump, plankton nets, sediment traps, box- and piston cores. For the present study, nine samples representing different environments sampled by different gear were selected: two plankton pump samples taken during the southwest monsoon of 1992; one from the centre of coastal upwelling and another from a gyre margin; one surface (28–13 m) and a deep water plankton net (1000–898 m) taken during the NE monsoon of 1993; two samples from a sediment trap, representing the upwelling maximum of August 1992 and the non-upwelling conditions of February 1993; one Recent ocean floor sample (box-core top) and two piston core samples, one representing the Younger Dryas and the other the Last Glacial Maximum (Figs. 1–3; Table 1). All samples are from NIOP station/site 905 off Somalia, except for the two plankton pump samples which were taken at stations off Oman (Fig. 1). Time control in the piston core was established by ^{14}C-AMS dating and oxygen isotope stratigraphy (Fig. 2). In Fig. 3 the method of sample preservation and processing is presented. The sieve mesh sizes used in this study are based on frequently used sieves in micropaleontologic studies, rather than choosing the size based on a mathematical relationship (e.g. an octave scale). The following sieve mesh sizes were used: 100, 125, 150, 180, 212, 250, 300, 355, 400, 450, 500, 560, 630 and 710 μm. The multinets used for the collection of the plankton samples have a mesh size of 100 μm. We used this size as a cut-off level for all samples. Thus, whenever percentages are given, they refer to the foraminifera larger than 100 μm. The dried residues of the size fractions were split with an OTTO microsplitter in order to obtain splits which contained approximately 300 specimens. In case less than 300 specimens were present in a size fraction, the whole fraction was counted. Planktic foraminifera were identified using a WILD M5A binocular microscope following the taxonomy of Bé (1967) and Hemleben et al. (1989). The samples did not show any signs of carbonate dissolution (i.e. contained well preserved whole pteropods).

3. Methods

3.1. Normalizing the data

Although individual foraminiferal shells show a stepwise chamber growth during ontogeny (Signes et al., 1993), the test size of a whole planktic foraminifer population can be represented by a continuous curve or density function (Fig. 4b). For the best possible approximation of the real size frequency distribution (SFD), in our case of foraminifera larger than 100 μm, normalization of the data is needed to remove the effect of unequal partitioning of the size spectrum (see Blanco et al., 1994). The normalized number of foraminifera per size interval, j, is obtained by dividing the percentage of foraminifer specimens of a certain species (Nf_j) by the size interval width. In this paper, the normalized number is given per nominal 25 μm:

$$\mathrm{Nfnorm}_j = \frac{25\mathrm{Nf}_j}{\mathrm{UL}_j - \mathrm{LL}_j} \quad (1)$$

where UL_j and LL_j are, respectively, upper and lower limit (in μm) of size interval j. For each size fraction, the number of specimens per nominal 25 μm interval is plotted against the size class geometric mean (GM) (Fig. 4). The choice of other mesh sizes would yield different numbers per size fraction but would not drastically change the shape of the normalized curve (Blanco et al., 1994).

3.2. Size frequency distributions (SFDs)

The test size of a planktic foraminifer species may graphically be represented in two ways: (1) by

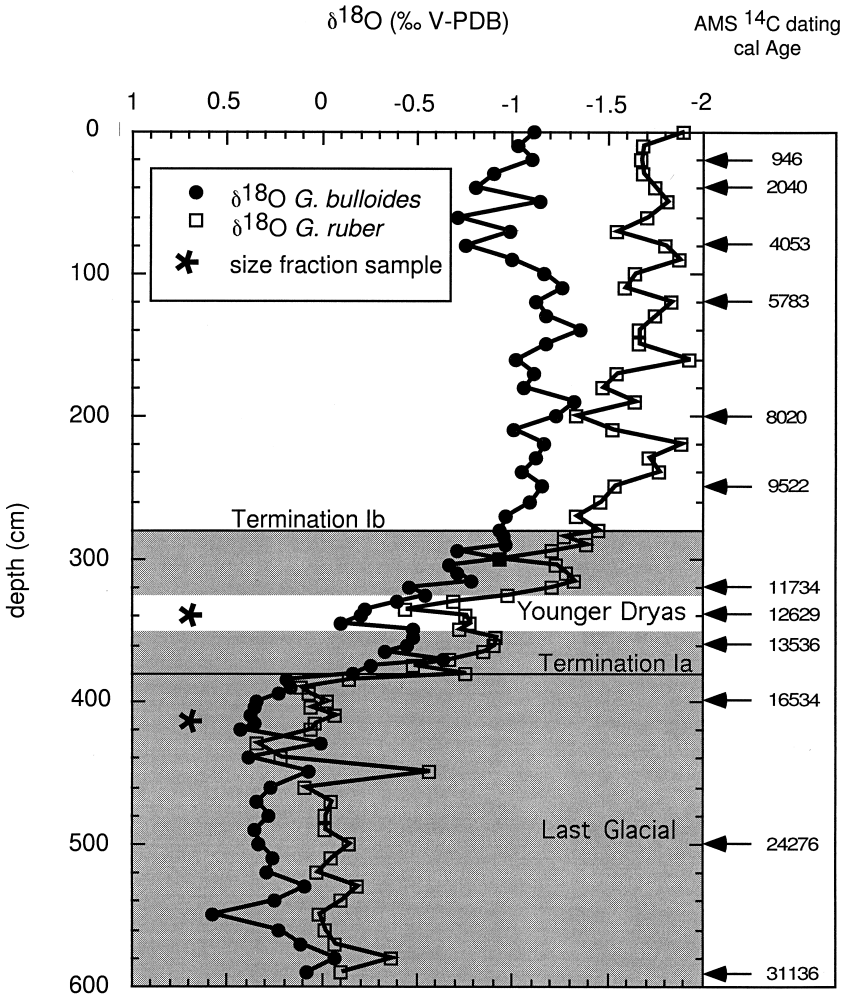

Fig. 2. Oxygen isotope curve of piston core 905P based on *G. bulloides* and *G. ruber* (after Ivanova et al., unpubl. data). Sample 905p/340 cm from the Younger Dryas, sample 905p/415 cm from the Last Glacial Maximum.

its SFD, which reflects the density of a species test size along the size spectrum; and (2) by plotting its cumulative size frequency (CSFD). For each SFD a CSFD can be plotted, as is shown for *G. bulloides* in Fig. 5a–f. Because we studied foraminifera larger than 100 μm, we define that all specimens of a species larger than 100 μm equal unity. Thus, one can read from the CSFD the median size, as well as the number of specimens present in any part of the size spectrum, as a fraction of all specimens larger than 100 μm.

3.3. Mathematical description of SFDs

The SFD of a foraminiferal species is described in this study by an exponential distribution, a Gaussian distribution, or by the sum of both. The two kinds of distributions are necessary in order to fit the size distributions of pre-adult (exponential) and adult specimens (Gaussian) accurately. The separate components of the SFDs can be used to estimate the relative contribution of pre-adult and adult specimens to the different size fractions. The method is illustrated using the data of *G. sacculifer* from the non-upwelling sediment trap sample (Fig. 4a–c)

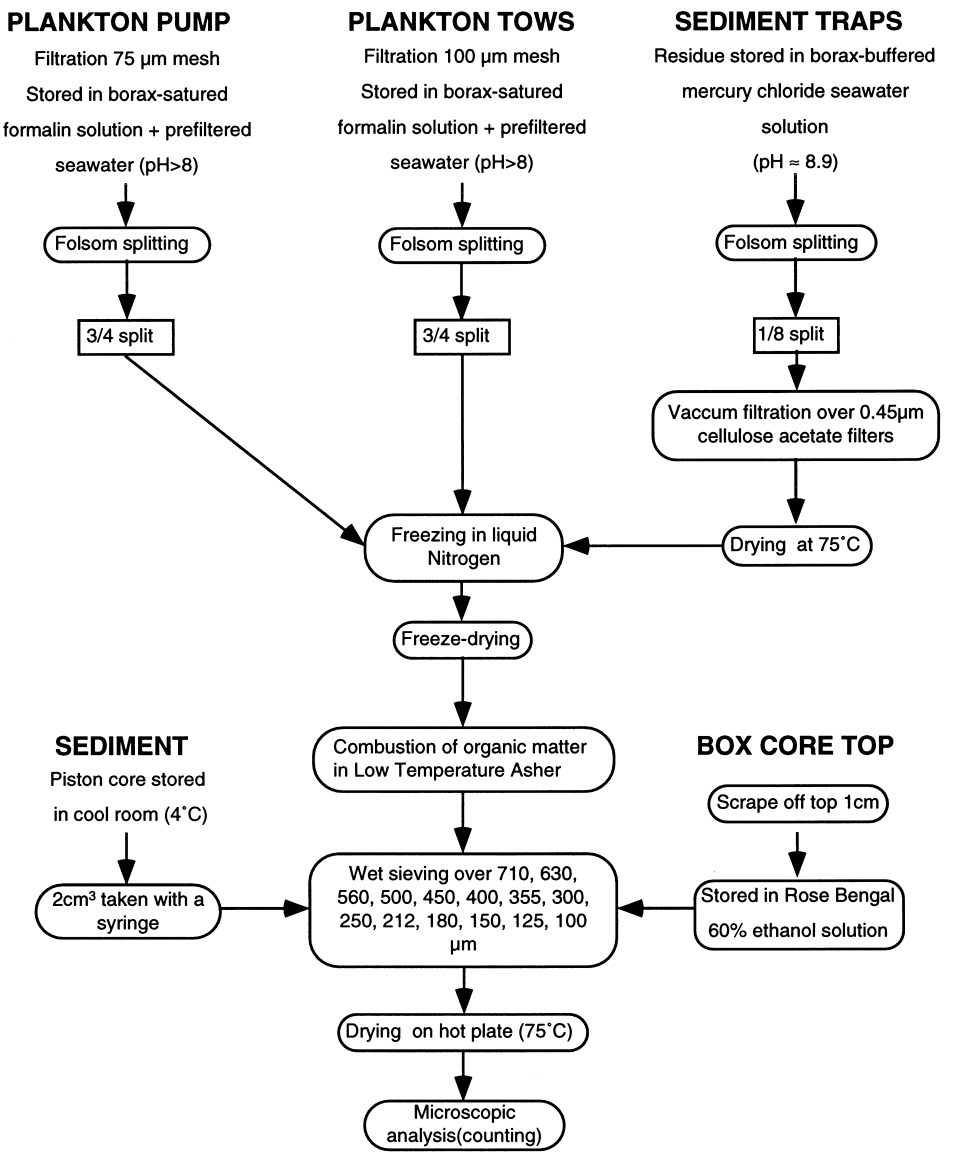

Fig. 3. Sample processing scheme.

applying the following equation to the data:

$$\mathrm{Nfnorm}(S) = C_1 \exp\left(-\frac{(S-100)}{C_2}\right) + \frac{C_3}{C_5\sqrt{2\pi}} \exp\left[-0.5\left(\frac{S-C_4}{C_5}\right)^2\right] \quad (2)$$

in which C_1, C_2, C_3, C_4 and C_5 are constants and S is the sieve mesh size in µm. The first part of the equation describes the exponential part of the SFD, in which C_1 is a scaling factor and C_2 describes the curvature. The second part, the Gaussian distribution, is described by three constants: C_3 equals the area under the curve, C_4 is the centre of the distribution and C_5 represents the standard deviation. Because the Gaussian shaped curve is symmetrical, C_4 also represents the average, modal and median size of the distribution of the adult population (Fig. 4c). Similar

Table 1
An overview of the samples used in this study

NIOP sample code	Type of the sample	Location	Date/period	Lunar day	Water depth	Remarks
C1-F29	plankton pump	16.09°N 52.31°E	August 20, 1992	7	approx. 3 m	upwelling/off Oman coast centre of upwelling/diatom bloom
C1-F37	plankton pump	15.40°N 52.58°E	August 23, 1992	10	approx. 3 m	upwelling/off Oman coast gyre margin/zooplankton bloom
905-4-4	plankton net	10.48°N 51.58°E	February 15, 1993	9	28–13 m	site 905/off Somalia non-upwelling/NE monsoon
905-1-1	plankton net	10.46°N 51.57°E	February 13, 1993	7	1000–898 m	site 905/off Somalia non-upwelling/NE monsoon
MST8-B5	particle flux sediment trap	10.45°N 51.57°E	from July 19 to August 2, 1992	6–20	1265 m	site 905/off Somalia upwelling/SW monsoon
MST8-B20	particle flux sediment trap	10.45°N 51.57°E	from February 1 to February 14, 1993	25–8	1265 m	site 905/off Somalia non-upwelling/NE monsoon
BC21WP7	sediment box-core top	10.46°N 51.58°E	Recent	–	1617 m	site 905/off Somalia
905P/340 cm	sediment piston-core	10.46°N 51.57°E	Younger Dryas	–	1567 m	site 905/off Somalia
905P/415 cm	sediment piston-core	10.46°N 51.57°E	Last Glacial Maximum	–	1567 m	site 905/off Somalia

to Eq. 2, a three component distribution consisting of a combined exponential and two Gaussian curves is described using:

$$\mathrm{Nfnorm}(S) = C_1 \exp\left(-\frac{(S-100)}{C_2}\right) + \frac{C_3}{C_5\sqrt{2\pi}} \exp\left[-0.5\left(\frac{S-C_4}{C_5}\right)^2\right] + \frac{C_6}{C_8\sqrt{2\pi}} \exp\left[-0.5\left(\frac{S-C_7}{C_8}\right)^2\right] \quad (3)$$

in which C_6, C_7 and C_8, represent scaling factor, centre and standard deviation of the second Gaussian distribution, respectively.

3.4. Average test size

The average test size of a foraminiferal species is calculated using the sieve size class middle value and the number of specimens per size fraction. The average test size calculated using sieves is comparable to an average test size calculated using the lengths of the intermediate axis of the foraminiferal shells. Often, the maximum test size diameter is used in average test size calculations, which thus results in a larger average test size. In this study we calculate an average test size of specimens larger than 150 μm (CLIMAP sieve size standard) using:

$$S_{\mathrm{av}} = \frac{\sum_{j=1}^{n} \mathrm{Nf}_j \sqrt{\mathrm{UL}_j * \mathrm{LL}_j}}{\sum_{j=1}^{n} \mathrm{Nf}_j} \quad (4)$$

in which Nf_j is the number of specimens present in fraction j, and UL_j and LL_j are, respectively, upper and lower limit of fraction j. Note that we used the geometric mean as a single value that represents the whole size class. Different values have been used as nominal sizes, e.g. the lower limit, the geometric mean or the arithmetic mean of size fractions. Generally the number of foraminiferal tests increases with decreasing size. Consequently, the size of foraminiferal tests within a size fraction will be closer to the lower limit than to the upper limit of that size fraction. The geometric mean will thus be a better single value that represents the whole size class that the arithmetic mean. However, because we used relatively narrow sieve size classes, changes in the inferred SFDs and calculations of average size, caused by either taking the arithmetic or the geometric mean of the size class, were extremely small, i.e. in the order of a few microns.

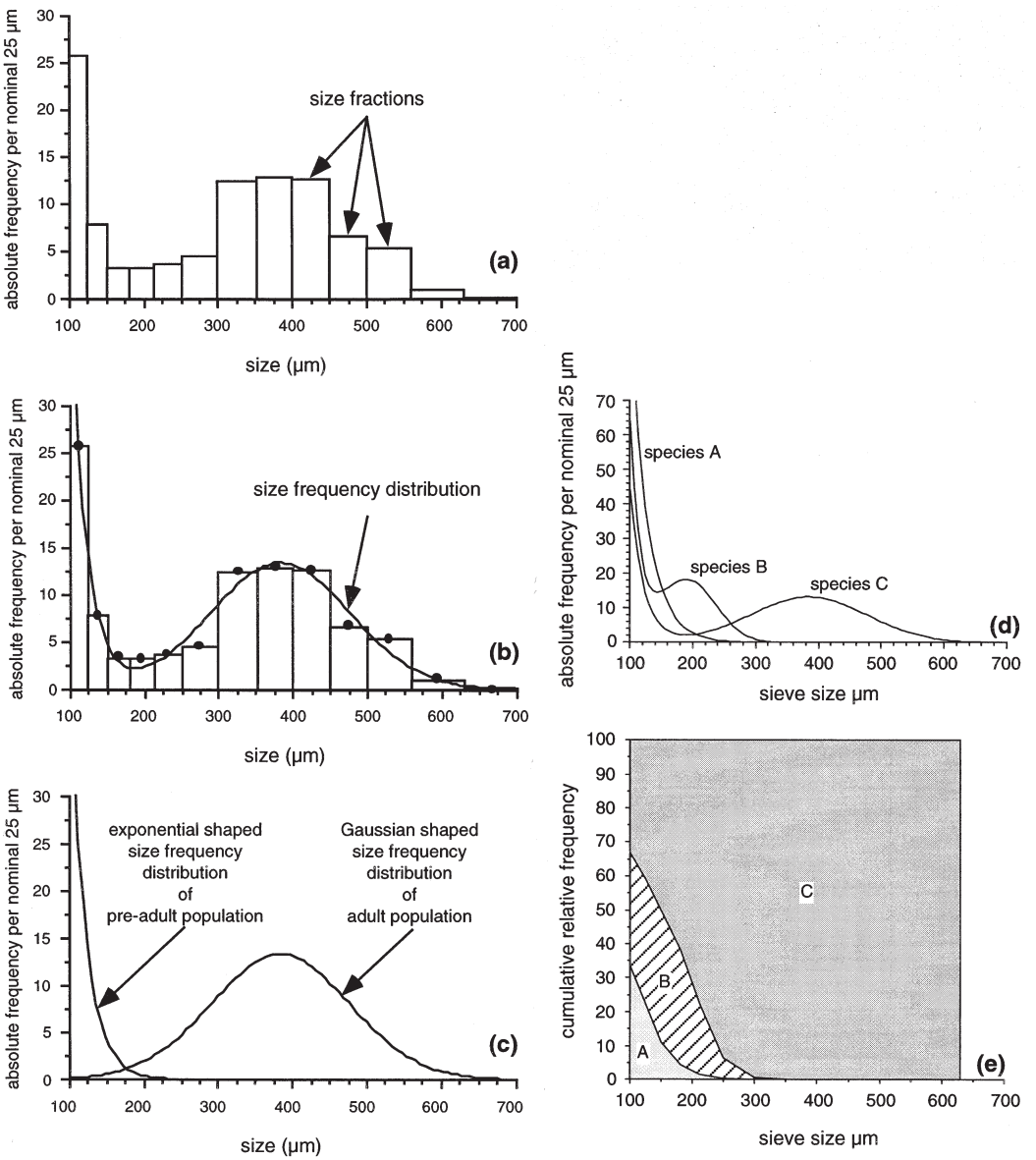

Fig. 4. Constructing the size frequency distribution (SFD) of a planktic foraminifer species from sieve fractions involves three steps (a–c): (a) The normalized frequency per size fraction is plotted. Normalization of the data is needed when the width of the size fractions used is not constant. (b) A size frequency distribution for the whole population is obtained by curve fitting. Here, the sum of an exponential and Gaussian distribution is used to fit the data. The size of foraminifera within a size fraction is represented by a single value: the size fraction's mean. (c) Size frequency distributions of pre-adult and adult shells are given separately. The sum of both separated distributions yields the size frequency distribution of the whole population (data shown are that of *G. sacculifer* from non-upwelling trap sample). (d) A hypothetical sample containing various species (*A*, *B*, *C*) with different size frequency distributions, will cause a changing relative abundance of the separate species as a function of sieve mesh size (e).

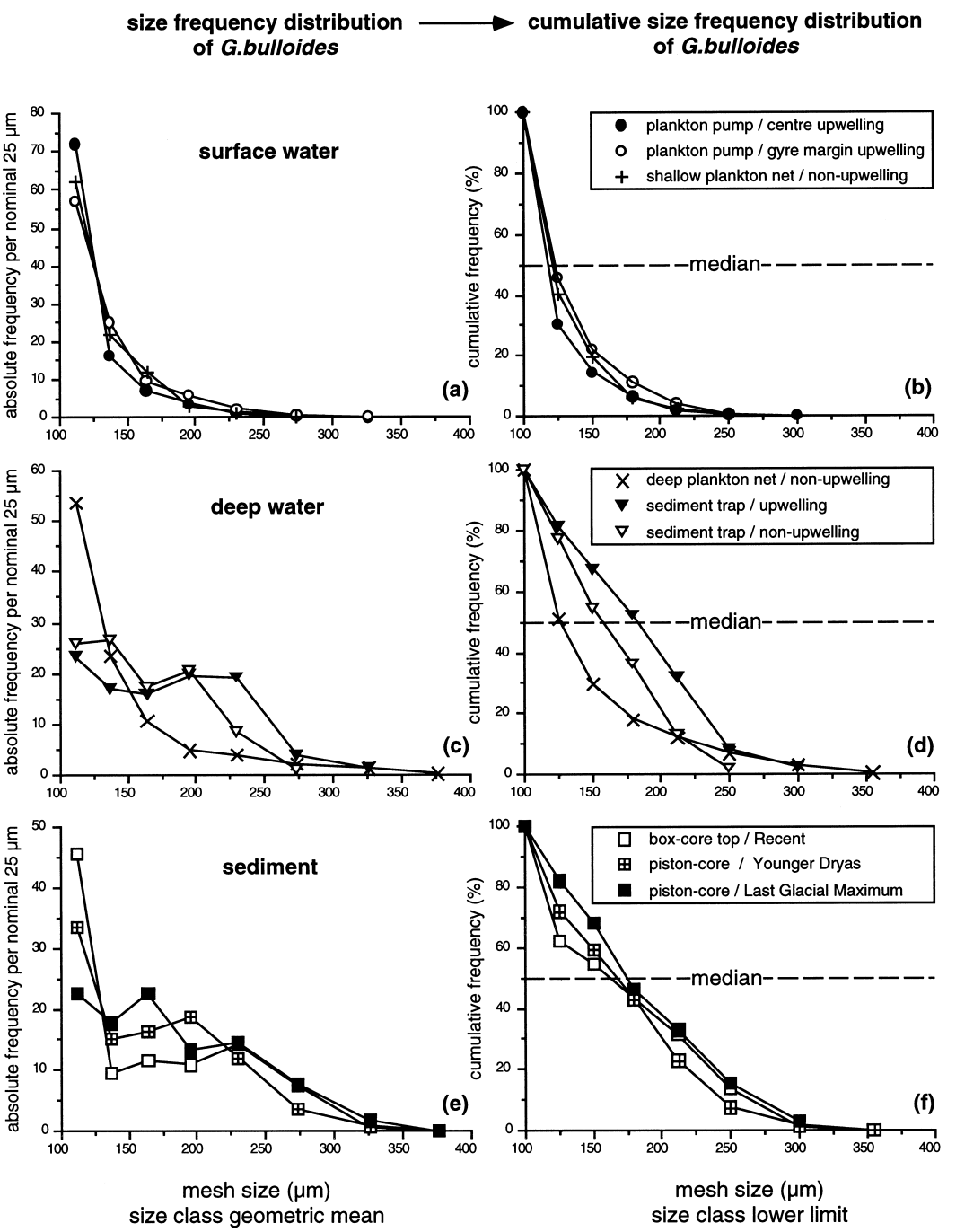

Fig. 5. Size frequency distribution (SFD) and cumulative size frequency distribution (CSFD) of *G. bulloides* in surface waters (a–b), deep water plankton net and sediment traps (c–d) and in the sediment (e–f). Note smaller median size at 50% in the cumulative graphs for living/surface water *G. bulloides*.

3.5. Species richness, Shannon diversity and equitability

In order to identify the effect of the sieve mesh size cut off level on the faunal composition, we have studied relative abundance of species as well as species richness (S), the Shannon diversity (H') and equitability (E') (Buzas and Gibson, 1969; Lipps et al., 1979) as a function of size. The Shannon diversity and equitability have been used as tracers of ocean environments (e.g. Ottens, 1992). Species richness is given by the number of species present in a sample. The Shannon diversity takes into account the proportion to which individual species are present:

$$H' = \sum_{i=1}^{S} p_i \ln p_i \quad (5)$$

in which S is the number of species and p_i the proportion of the ith species. In the literature different log bases have been used, which can easily be compared by multiplying by a constant.

Equitability (E') gives information on the similarity between species proportions and ranges in value from 0, when the assemblage consists of a single species, to a value of 1 when all species are present in the same proportion:

$$E' = \frac{e^{H'}}{S} \quad (6)$$

in which H' is the Shannon diversity and S the species richness. To show the effect of the sieve cut-off level on the relative abundance, the data are plotted cumulatively starting with the largest sieve (Fig. 4e–f). For each sieve fraction used, the fauna present in all larger fractions is added and the relative abundance of the species is (re)calculated. For example, the >450 μm relative abundance of species is based on the sum of the counts in fractions: 450–500, 500–560, 560–630, 630–710 and >710 μm.

3.6. Equivalent catch

Since smaller mesh sizes of sieves and plankton nets result in a larger number of foraminifera per sample, the mesh size choice leads to incomparable numbers of foraminifera and species proportions. Berger (1969) introduced the concept of equivalent catch to compare the concentrations of living foraminifera collected with plankton nets of unequal mesh size. In his example, a 70 μm mesh phytoplankton net catching 160 specimens and a 300 μm zooplankton net catching 2 specimens in the same volume of water yield the same equivalent catch of 16 specimens at his standard net size of 158 μm. He concluded that the concentrations of living foraminifera reported by various workers can be standardized according to:

$$\text{Nf (equivalent)} = \text{Nf (actual)} \left(\frac{M_a}{M_s} \right)^{\alpha} \quad (7)$$

where M_a is the actual mesh opening used (net mesh size or sieve mesh size) and M_s is the standard mesh size. Rewriting Eq. 7 in order to describe the total number of foraminifera found at sieve mesh size M_a yields:

$$\text{Nf (actual)} = \text{Nf (equivalent)} \left(\frac{M_s}{M_a} \right)^{\alpha} \quad (8)$$

Berger (1969) used $\alpha = 3$ for plankton tow samples. Straightforward use of Eqs. 7 and 8, with $\alpha = 3$, to samples from different environments would overestimate the numbers of large foraminifera in our (extreme) plankton pump samples as a result of relatively abundant small *G. bulloides* and underestimate the number of relatively large foraminifera present in sediment trap and sediment samples. Consequently the value of the exponent α is not constant and varies with the kind of sample. In this paper we use Eq. 8 to describe the total number of foraminifera as a function of sieve mesh size, using Nf (equivalent) = 100 and M_s = 100 μm. The number of foraminifera found at any sieve mesh size is expressed as a fraction of the foraminifera >100 μm. A best fit curve fitting procedure yields values for the exponent α for different environments.

4. Results

4.1. Size frequency distributions of G. bulloides

The SFDs of *G. bulloides* are very similar in the shallow plankton net and both plankton pump samples, although they were taken during upwelling and

non-upwelling conditions. In surface waters SFDs show an exponential relationship with highest density in the lower part of the size spectrum (Fig. 5a). The CSFD shows that 15–22% of the standing stock (>100 μm) is present in fractions larger than the CLIMAP standard of 150 μm and consequently 78–85% is present between 100 and 150 μm (Fig. 5b).

The samples from the deep water include a deep plankton net and two sediment trap samples, one reflecting upwelling conditions of August 1992, the other the non-upwelling conditions in February 1993, when the ocean was stratified and a deep chlorophyll maximum was present (Brummer, 1995). The non-upwelling trap sample and the deep plankton net were taken from the same locality at the same time, hence they can be used to compare the SFDs of species in the water (concentration) to those which were collected by a sediment trap at 1265 m water depth (flux). The SFD of *G. bulloides* from the deep plankton net shows a similar exponential trend as observed in surface water distributions (Fig. 5a, c). The CSFD shows that 30% of the specimens are larger than 150 μm, which is an increase of 10% compared to the surface water plankton from the same station (Fig. 5d). In both sediment trap samples the SFDs of *G. bulloides* are not continuously decreasing with size and show a maximum in the density distribution at 195 μm (Fig. 5c). Consequently, these specimens are, on average, larger than those collected in surface waters, and the CSFDs show that 54% (non-upwelling) and 68% (upwelling sample) is larger than 150 μm, respectively (Fig. 5d). The SFDs of *G. bulloides* in sediment samples (Fig. 5e) mirror the distributions of *G. bulloides* in the sediment trap samples. They are characterized by a local density maximum in the larger part of the size spectrum and an increasing shell density in the lower part of the size spectrum. Apart from small differences in the SFDs of *G. bulloides* from the sediment samples, the general shape of the curve remains. We consider these SFDs to consist of two components: (1) an exponential distribution of relatively small immature specimens; and (2) a Gaussian shaped distribution reflecting larger specimens which reached the adult/terminal stage and had probably reproduced. The CSFDs of *G. bulloides* in the sediment samples show that 55–68% of the specimens are larger than 150 μm (Fig. 5f).

Fitting Eq. 2 to the data yields a maximum value of the Gaussian distribution at 210 μm in the Recent sediment, representing the average, median and modal size of the adult/gametogenetic population (Fig. 6a). In the Younger Dryas and the Last Glacial Maximum the modal size of adults is found at 190 and 154 μm, respectively, and adult specimens are thus smaller on average (Fig. 6b–c).

Because the average test size of foraminifera is a common proxy used in paleoceanographic studies, we wanted to test whether the average test size obtained by curve fitting, viz. the modal size of the Gaussian curve, equals the average test size calculated using Eq. 4. The average test size of *G. bulloides* in both the Recent and the Younger Dryas as calculated using Eq. 4, is close to the modal size found in the Gaussian shaped distribution (Fig. 6a–b). On the other hand, the average test size calculated for the Last Glacial Maximum is 61 μm below the modal size at 215 μm (Fig. 6c). Therefore, average size does not necessarily represent the modal size of adult *G. bulloides* and thus should be used with care.

4.2. Size frequency distributions of G. glutinata

The SFDs of *G. glutinata* (Fig. 7a–f) show that it is a relatively small species. Specimens in fractions above 400 μm are not recorded and highest densities are consistently found in the finest fractions. Again, SFDs are exponential in the water column (Fig. 7a), whereas in sediment trap (Fig. 7b–c) and core samples (Fig. 7d–f), a superimposed Gaussian distribution is recognized. Separating these distributions using Eq. 2 yields a modal size of adult *G. glutinata* specimens between 138 and 190 μm. In surface water only 6–16% of the *G. glutinata* specimens are larger than 150 μm, in the deep plankton net 12% are larger than 150 μm, in traps 33% (non-upwelling) and 44% (upwelling), and in the sediment 21–35%.

4.3. Size frequency distributions of G. ruber

In the Arabian Sea, *G. ruber* is the second most abundant species, dominating the assemblages in the northern and eastern regions where upwelling is less intense (Cullen and Prell, 1984; Zhang, 1985). In the surface water samples *G. ruber* shows an exponential

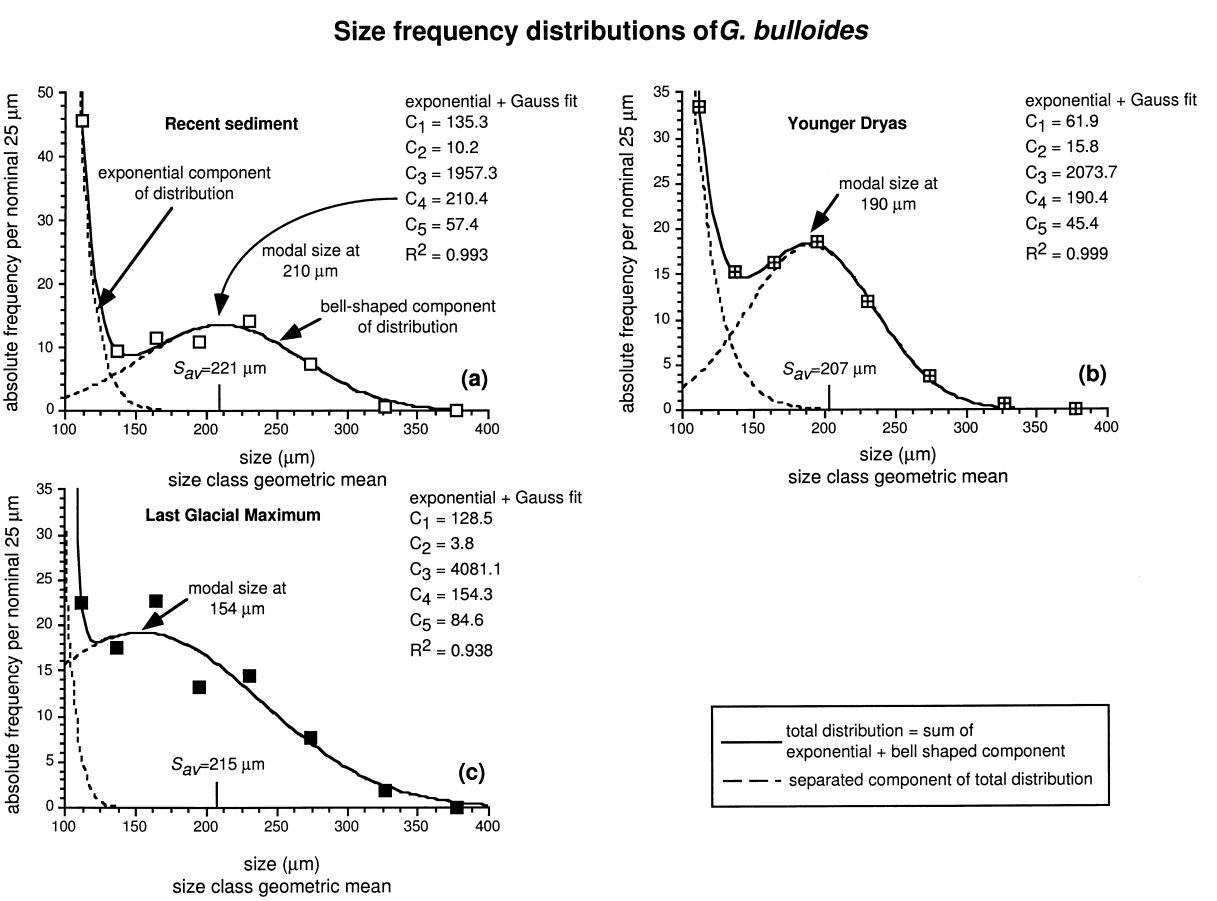

Fig. 6. Size frequency distributions of *G. bulloides* in sediment samples, showing that the total size frequency distribution consists of a pre-adult exponential component and a Gaussian-shaped component reflecting larger specimens in the adult stage of ontogeny. Note the shift in the modal size of the adult population from 210 µm in the Recent box-core top sample (a) to 190 µm and 154 µm in the Younger Dryas (b) and Last Glacial Maximum, respectively (c). The average test size of *G. bulloides* as calculated using Eq. 4 of all specimens >150 µm is indicated with S_{av}. Coefficients C_1 to C_5 are those of Eq. 2, C_4 represents the modal size of the adult population.

SFD (Fig. 8a). The SFD of *G. ruber* from the deep plankton net (Fig. 8b) shows that both pre-adult and adult specimens are present. The modal size of the adult population is 208 µm, which is close to the modal size of 199 µm observed in the sediment trap sample from the same location (Fig. 8c). In the sediment trap samples (Fig. 8c) the SFD shows a Gaussian distribution and, different from other species, does not show higher numbers reflecting pre-adult specimens in the finest part of the size spectrum. A modal size of approximately 195 µm is found in both the upwelling and the non-upwelling trap sample. Because both sediment trap samples show a unimodal distribution, we assume that pre-adult specimens of *G. ruber* are mostly present in fractions smaller than 100 µm. The SFD of *G. ruber* in the Recent sediment (Fig. 8d) shows a modal size of adult specimens at 207 µm and the pre-adult specimens restricted to fractions smaller than 125 µm. Adult specimens of *G. ruber* from the Younger Dryas and Last Glacial Maximum (Fig. 8e–f) are smaller, having a modal size of 139 and 169 µm, respectively. Pre-adults are virtually absent or restricted to fractions smaller than 125 µm.

In the surface water samples 23–27% of the *G. ruber* specimens are larger than 150 µm. In the deep plankton net this has increased up to 44% and in both trap samples 83% are larger than 150 µm. In

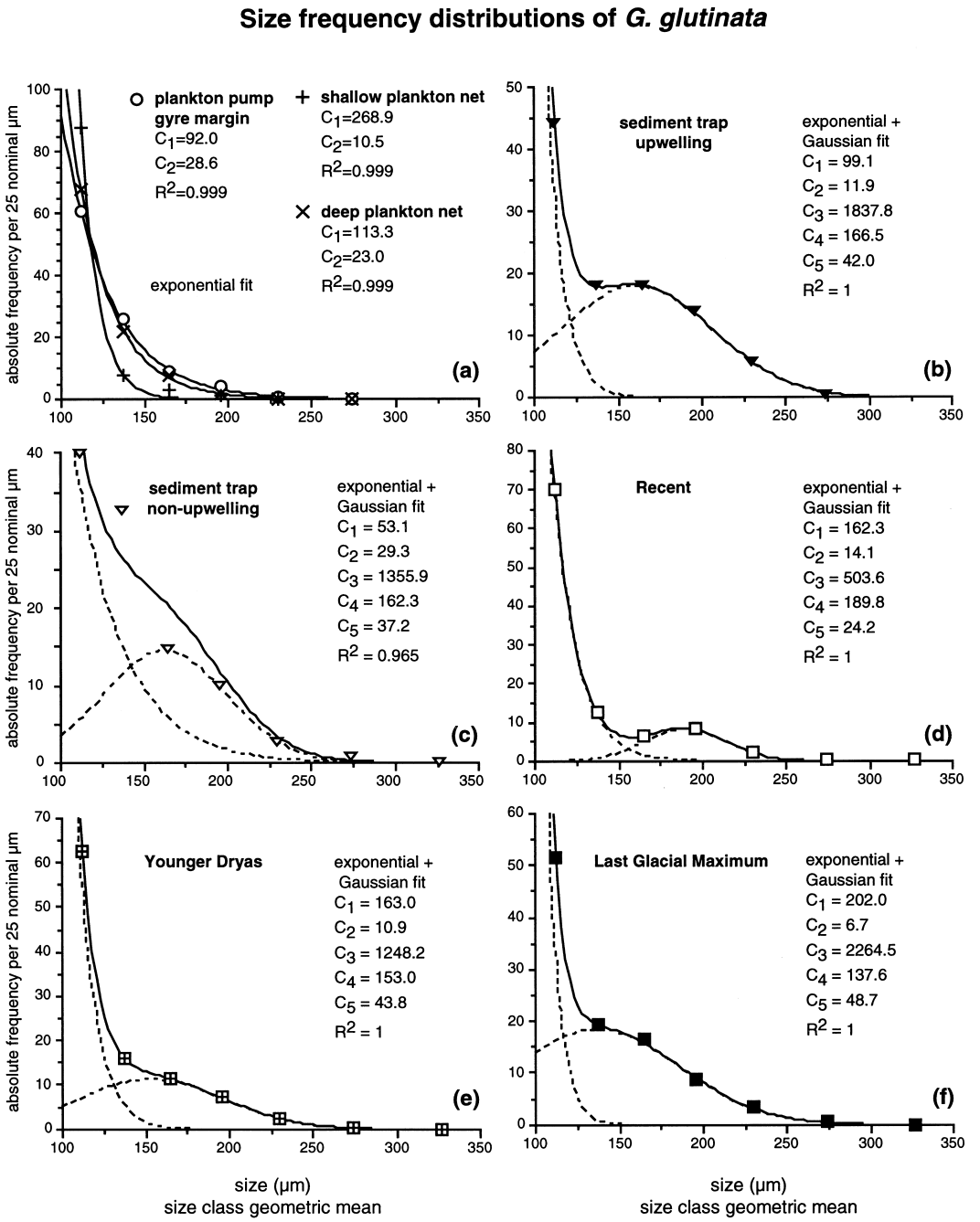

Fig. 7. Size frequency distributions of *G. glutinata* in all samples except the plankton pump sample from the centre of the upwelling, that contained too few specimens. Water column distributions have an exponential nature (a), whereas the sediment trap and sediment distributions are the sum of an exponential and Gaussian distribution (b–f). Highest densities are found in the smallest part of the size spectrum. The modal size of adult *G. glutinata* varies between 138 and 190 µm. Coefficients C_1 to C_5 are those of Eq. 2, C_4 represents the modal size of the adult population.

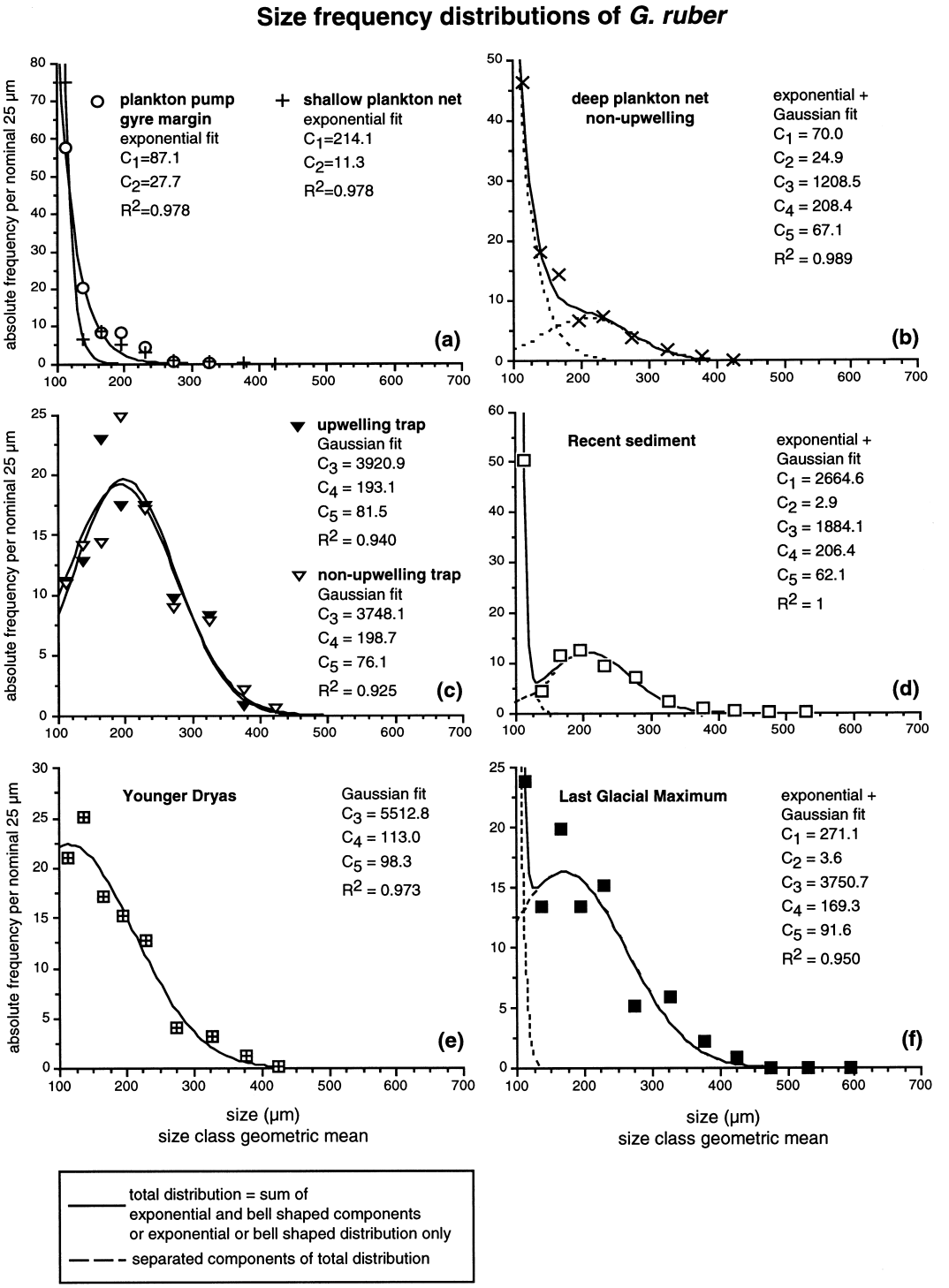

Fig. 8. Size frequency distributions of *G. ruber* in surface waters (a), the deeper part of the water column (b–c) and in the sediment (d–f). Surface water distributions have an exponential nature. Coefficients C_1 to C_5 are those of Eq. 2, C_4 represents the modal size of the adult population.

the sediment samples 55–72% are larger than 150 μm.

4.4. Size frequency distributions of G. sacculifer

G. sacculifer is commonly observed in living foraminiferal populations during periods of non-upwelling. This species is frequently used in laboratory culturing experiments and a relatively large data base is available on its ontogenetic and ecological behavior (Bé, 1980; Caron et al., 1981; Hemleben et al., 1989; Brummer and Kroon, 1988; Bijma et al., 1990, 1994; Erez et al., 1991; Bijma and Hemleben, 1994). It has been shown that test size variations of this species in the water column are related to the reproductive cycle, which appears to be related to lunar cycles (Bijma et al., 1990, 1994; Bijma and Hemleben, 1994). The species is thought to reproduce around full moon, resulting in higher fluxes of relatively large specimens at greater depth, while small specimens of the new population inhabit surface waters during the first weeks after full moon. Although our data do not represent a time series of samples which can be related to lunar cycles, our results show striking similarities with the results of Bijma et al. (1990, 1994) and Bijma and Hemleben (1994).

Following Bijma and Hemleben (1994), a normal-form (NOR) and sac-like morphotype (SAC) of *G. sacculifer* is distinguished. Their kummerform morphotype is included in the NOR group, and their kummersac morphotype (KUMSAC) in the SAC morphotype.

In the shallow plankton net sample (Fig. 9a) *G. sacculifer* shows an exponential SFD. Although highest numbers are found in the finest part of the size spectrum, some larger specimens are present up to fractions as coarse as 560–630 μm, possibly representing the relic population of *G. sacculifer* which has reproduced around the previous full moon. The SFD of *G. sacculifer* in the deep plankton net (Fig. 9b) clearly shows a Gaussian distribution of adult gametogenetic specimens with a modal size of 342 μm. All SAC and KUMSAC specimens are present in fractions larger than 300 μm. This sample was collected 7 days after full moon (Table 1) and thus mainly collected the empty shells of specimens that have reproduced around the previous full moon. The shallow plankton net (Fig. 9a) collected 9 days after full moon (Table 1) mainly consists of specimens of the new population as indicated by the exponential SFD. The SFD of *G. sacculifer* from the upwelling trap sample (Fig. 9c) collected from the 6 to 20th lunar day, shows that mainly pre-adult specimens were caught, while the SFD in the non-upwelling sediment trap sample (Fig. 9d), which collected specimens from the 25–8th lunar day and thus included a full moon, show abundant adult specimens. These observations match the results of a sediment trap simulation experiment of Bijma et al. (1994, p. 516, fig. 3b, d) with remarkably accuracy. The SFDs of *G. sacculifer* from the deep plankton net and non-upwelling sediment trap are very similar (Fig. 9b, d) and minor differences are the result of size depending settling velocity and have been caused by different timescales of sampling (20 minutes for the plankton net vs. 2 weeks for the sediment trap sample).

In the Recent sediment and Younger Dryas a modal size of 300 μm and 325 μm of *G. sacculifer* is found, respectively (Fig. 9e–f). The scatter in the SFD of *G. sacculifer* from the Recent sediment is due to the increasing number of shells in smaller size fractions and the combined low absolute abundance of *G. sacculifer* in these fractions, increasing the measurement error.

In the shallow plankton net 35% of the *G. sacculifer* specimens are larger than 150 μm, increasing to 85% in the deep plankton net. In the non-upwelling trap sample 80% are larger than 150 μm, against only 33% during upwelling. In the Younger Dryas sample 26% are larger than 150 μm.

4.5. Size frequency distributions of the dextral Neogloboquadrina *complex*

Morphologic gradation between dextral *N. dutertrei* and *N. pachyderma* often hinders assignment of the specimens to the correct species. They should not be lumped in one taxonomic category since the two species represent different geographical and ecological regions (Hilbrecht, 1997). Two groups of dextral *Neogloboquadrina* were identified: (1) *N. dutertrei*; and (2) *N. pachyderma* including the P–D intergrades (Plates I and II). Based on their morphology, adult *N. dutertrei* can be distinguished from *N.*

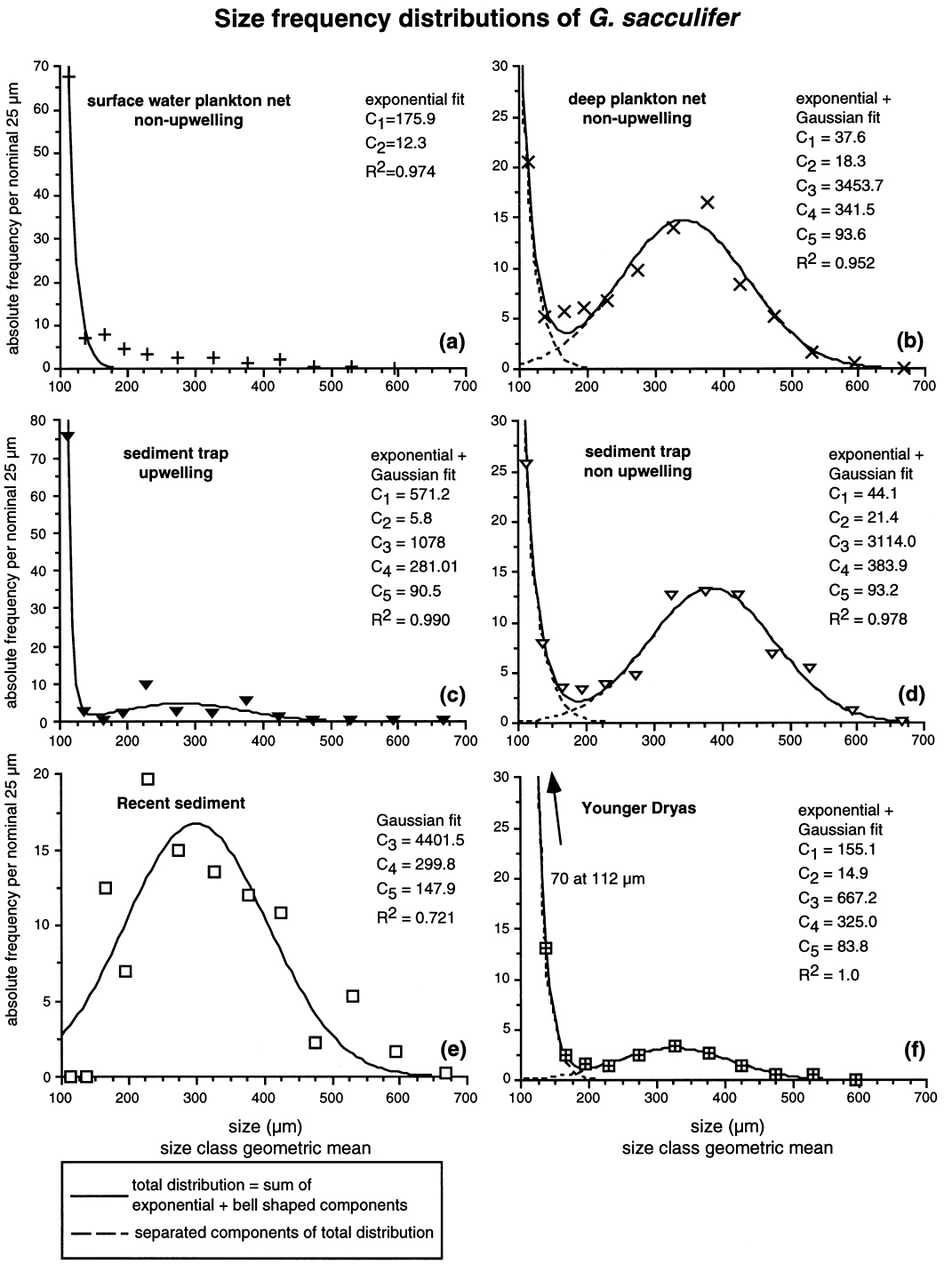

Fig. 9. Size frequency distribution of *G. sacculifer* in surface waters (a), the deeper part of the water column (b–d), from the Recent sediment (e) and Younger Dryas (f). Adult specimens of *G. sacculifer* show a pronounced modal size between 281 and 384 µm. The Gaussian distributions of adult specimens mainly reflects the SAC-like morphotypes, which underwent gametogenesis. Coefficients C_1 to C_5 are those of Eq. 2, C_4 represents the modal size of the adult population.

pachyderma by having a more lobulate periphery, an umbilical tooth, higher coiling and 4–6 chambers in the final whorl (Plate II). Representatives of the second group (*N. pachyderma* + P–D intergrades) were only present in fractions smaller than 400 μm. Consequently, a part of the *N. dutertrei* population, in particular morphologically indistinct sub-adult specimens, are included in the second group. Because this group is a mixture of the species, we used the curve fitting technique to separate the species, assuming that the separate distributions for adult *N. dutertrei* and *N. pachyderma* are unimodal Gaussian and their modal adult size is different. For this purpose both groups were lumped and SFDs of the dextral *Neogloboquadrina* complex (combined groups 1 and 2) were plotted (Fig. 10a–g).

The SFDs of the dextral *Neogloboquadrina* complex follow an exponential trend in samples from surface water and the deep water plankton net (Fig. 10a–b), and show a bimodal pattern in the trap and sediment samples (Fig. 10c–g). Both trap samples show two maxima, the first between 150 and 200 μm and the second around 330 μm (Fig. 10c–d). The bimodal SFD was fitted using Eq. 3, yielding two well defined Gaussian curve maxima in both sediment trap samples. In the upwelling trap sample (Fig. 10c) the first maximum is found at 182 μm and the second at 339 μm. In the non-upwelling trap sample (Fig. 10d) these maxima are found at 139 and 319 μm, respectively. The widths of the smaller and larger Gaussian distributions, are similar in both samples (note that C_5 and C_8 represent the widths of the smaller and larger distributions, respectively). The two Gaussian distributions in the sediment samples center between 165 and 201 μm and between 311 and 363 μm, respectively (Fig. 10e–g).

Kroon and Darling (1995) reported a multimodal size frequency distribution of *N. dutertrei* from a glacial Panama Basin sample. They related this to the presence of different populations of the species and showed that the oxygen isotopic composition of the smaller population is at least 1 per mil lighter than the larger one. On the other hand, the same authors report that cultured specimens of *N. dutertrei* are all pre-gametogenetic below 360 μm, suggesting that the smaller population is exclusively pre-gametogenetic. However, taking into account the taxonomic difficulties associated with both species, especially in smaller size fractions, and the consistent bimodal SFD of the dextral *Neogloboquadrina* complex (Fig. 10c–g), we suggest that two species rather than two populations of one species are involved. A cross check with the observations of the separate groups showed that the larger distributions only contained *N. dutertrei* specimens (Plate I, 1, 2; Plate II, 1, 2). Consequently, the smaller peak is assumed to be attributed to dextral *N. pachyderma*.

The Last Glacial Maximum sample shows a much higher abundance of the *N. pachyderma* population than the *N. dutertrei* population, whereas in the Recent sediment *N. dutertrei* is more abundant than *N. pachyderma*. This observation is consistent with previous studies, showing that dextral *N. pachyderma* is more abundant in the Last Glacial than in the Recent (e.g. Naidu and Malmgren, 1996a).

4.6. Faunal changes as a function of sieve size

In order to investigate the effect of the sieve mesh size cut off level on the faunal composition, we studied the relative abundance of species as well as species richness (S), the Shannon diversity (H') and equitability (E') as a function of size (Buzas and Gibson, 1969; Lipps et al., 1979).

4.6.1. Relative abundance

Previous work showed that the species composition differs between size fractions of the same sample (Berger, 1971; Bé and Hutson, 1977; Brummer and Kroon, 1988). Larger size fractions consist of what are commonly considered to be relatively warm faunas, the smaller fractions are composed of relatively cold faunas (Bé and Hutson, 1977). Many statistical techniques often use percentage data of the faunal assemblage. For a sediment sample from Santa Barbara Basin, Berger (1971) showed that the probable surface water temperature as calculated using average specific values, dropped by approximately 3ºC from 17 to 14ºC, using the fauna composition from >250 μm down to 62 μm.

In our samples the relative abundance of species changes strongly with size (Fig. 11); the coarser part of the size spectrum is dominated by *O. universa* and *G. menardii*, whereas *G. sacculifer, N. dutertrei* and *P. obliquiloculata* dominate the middle part of the spectrum. *G. bulloides*, which is always abundant in

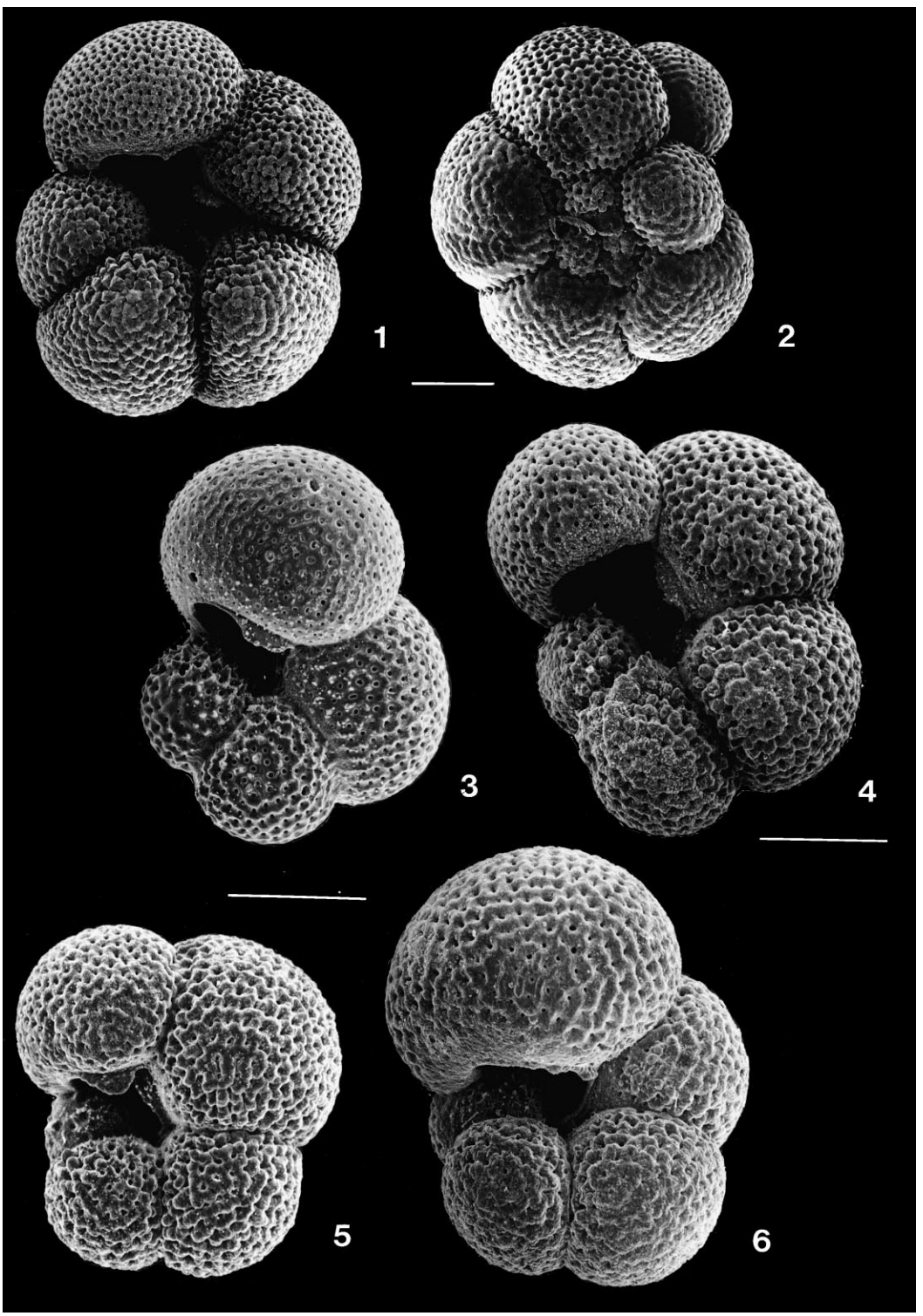
1
2
3
4
5
6

sediment samples, suppresses the relative contribution of other species below 300 μm (Fig. 12). In turn, the increased abundance of *D. anfracta, G. glutinata, T. quinqueloba, T. iota, N. pachyderma* (sin.) and the increasing number of pre-adult specimens of larger species, cause a relative decrease of *G. bulloides* in the finest part of the spectrum.

4.6.2. Species richness, Shannon diversity and equitability

The species richness (S), Shannon diversity (H') and equitability (E') as a function of sieve mesh size are plotted in Fig. 12a–c. Generally, species richness and the Shannon diversity increase with decreasing sieve mesh size, while equitability decreases with decreasing mesh size and is relatively constant below approximately 200 μm.

Both plankton pump samples only contain foraminifera smaller than 355 μm and the Species richness is low, ranging from 15 for the centre upwelling sample to 17 in the gyre margin (Fig. 12a). The Shannon diversity is 1 at 100 μm and is consistently higher throughout the size spectrum in the gyre margin sample, reflecting a little more balanced fauna composition (Fig. 12c). Both of these pump samples are strongly dominated by the species *G. bulloides*, which accounts for approximately 80% of the total fauna as reflected in the low equitability values (Fig. 12b). In the shallow plankton net (non-upwelling), Species richness is nearly equal to the plankton pump samples (17 species), but the assemblage is less dominated by one species as shown by a higher Shannon diversity and equitability values (Fig. 12a–c).

The deeper water, as sampled by the deep plankton net and the two sediment trap samples, is characterized by higher Species richness and Shannon diversity values than surface water samples (Fig. 12a, c). The Shannon diversity reaches a local maximum of around 2.08 in the upwelling trap sample at a sieve mesh size of 250 μm and drops to 1.95 at a mesh size of 180 μm. The Shannon diversity decreases between approximately 150 and 300 μm in all *G. bulloides*-rich samples (Fig. 12c). The SFDs of *G. bulloides* (Figs. 5 and 6) show that this species is consistently present in fractions smaller than 300 μm and reaches an adult size between 150 and 250 μm, thus suppressing the relative contribution of other species and hence decreasing the Shannon diversity. Below 150 μm the Shannon diversity generally increases again due to the contribution of small species.

At sieve mesh size 100 μm both the Recent assemblage and the fossil core assemblages show a high Species richness of 27–29 species and a Shannon diversity of 2.3 to 2.5 (Fig. 12a, c).

4.6.3. Total number of foraminifera as a function of sieve size

Foraminifera larger than 250 μm are virtually absent in the upwelling plankton pump samples, whereas in the other samples 6–13% of the foraminifera are larger than 250 μm. An exception to this is the non-upwelling February sediment trap sample which contained more than 22% foraminifera larger than 250 μm. The total number of planktic foraminifera changes along the size spectrum in all studied samples and is highest in its finest part (Fig. 13; Table 2). In plankton pump and plankton net samples 59–73% of the planktic foraminiferal assemblage is present in the finest 100–125 μm fraction and 75 to 87% is present between 100 and 150 μm (Table 2). The finest fraction of the trap samples has 48% for the upwelling trap sample and 29% for the non-upwelling trap sample. Adding the 125–150 μm fraction, respectively 59% and 47% of the foraminifera are present between 100 and 150 μm. The number of foraminifera in the finest fraction of the sediment samples is relatively constant at 49–57% for the 100–125 μm fraction and 63–68% for 100–150 μm.

We used Eq. 8 to calculate best fits, describing the total number of foraminifera as a function of the sieve mesh size, and found that α ranges from 1.8 for

---

Plate I

All specimens from the upwelling sediment trap sample. Scale bar = 100 μm.

1–2. Adult *Neogloboquadrina dutertrei* from size fraction 355–-400 μm.
1. Umbilical view.
2. Spiral view.
3. *Neogloboquadrina dutertrei* from size fraction 212–250 μm, umbilical view.
4–6. P–D intergrades from size fraction 212–250 μm, umbilical views.

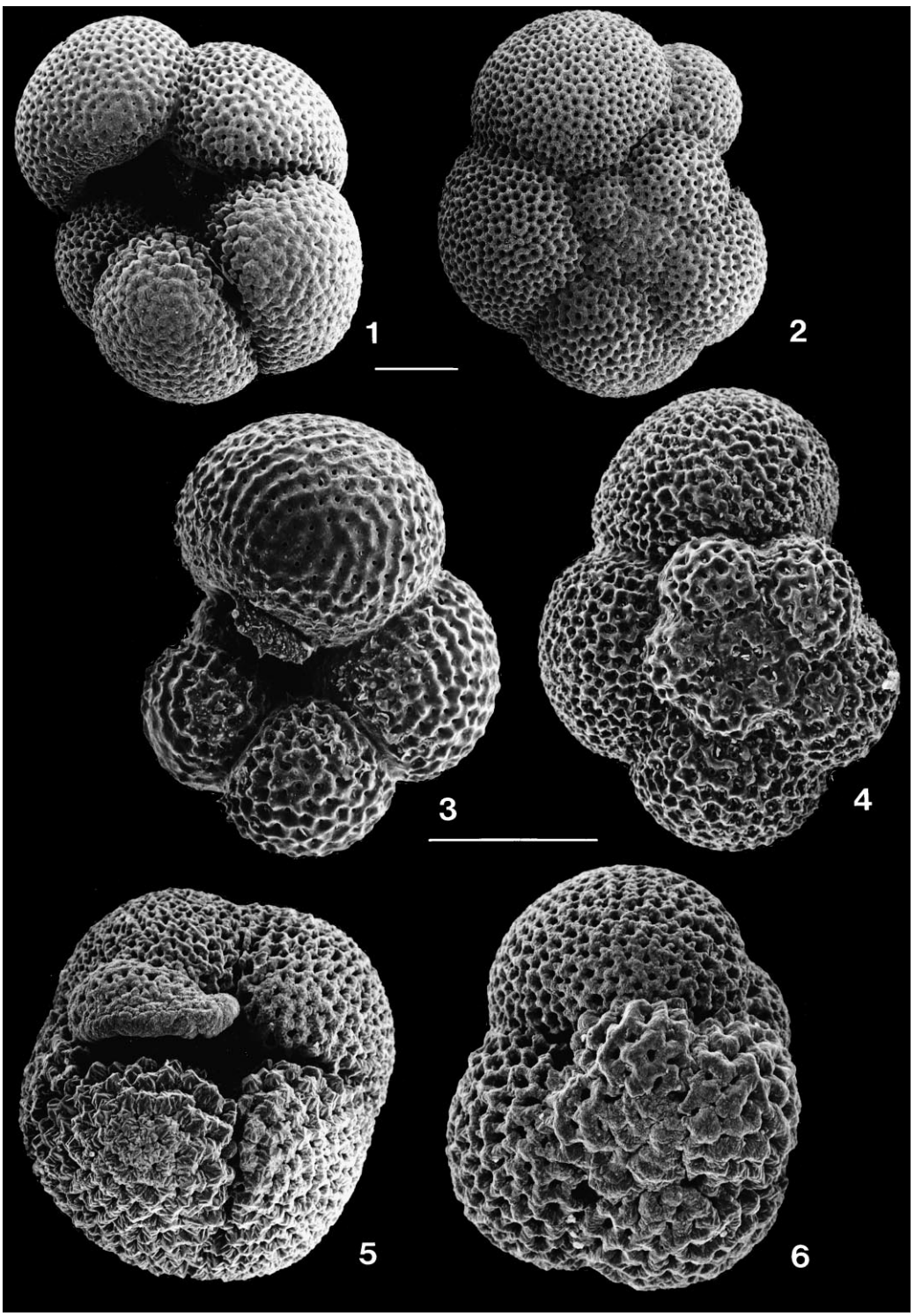
1
2
3
4
5
6

the sediment trap non-upwelling sample to 5.6 for the plankton pump core upwelling sample (Fig. 13). In general, values for α between 3.5 and 5.6 are related to assemblages from plankton pump and nets, whereas values ranging between 1.8 and 3.0 are related to settling flux samples and fossil faunas in sediment trap and sediments assemblages. All curve fits have r^2 of 0.98 or higher and fit the data very well between 100 and 400 μm. The distinct difference in α values for concentrations of foraminifera in the water column (pump and plankton nets) and for settling flux samples (traps and sediment) is the result of changes in the ratio between the number of relatively large adult species dominating settling flux assemblages, versus small species and small pre-adult specimens of larger species which dominate in watercolumn assemblages. Because of this, α may be a time dependent size parameter, tied to the ontogenetic development of living populations, or may serve as a measure for dissolution or winnowing in fossil faunas.

5. Discussion

5.1. Species size frequency distributions

The total number of foraminifera as a function of sieve mesh size is determined by two characteristics of the faunal assemblage: (1) the absolute abundance of the constituent species; and (2) their size frequency distributions. We found that species SFDs vary between samples. Generally, SFDs of living planktic foraminifera in surface waters follow an exponential trend, whereas their export fluxes may show a superimposed Gaussian shaped distribution reflecting larger adult specimens. The SFDs vary according to the type of sample studied, e.g. plankton (pump, net), settling flux (deep net, sediment trap), or a fossil assemblage (box, piston-core). In addition, SFDs of species from plankton and settling flux assemblages are affected by the ontogenetic stage in which a population is at the time of sample collection: e.g. Schiebel et al. (1997) showed that many small tests of *G. bulloides* in the North Atlantic were present during the first half and at the end of the lunar cycle, whereas large numbers of large tests were found in the first week after full moon.

5.2. Processes controlling the variability of SFDs

The SFDs of species are controlled by various factors:

(1) The physical and chemical conditions of the surface water directly control the population dynamics of planktic foraminifera and thus their size distribution. Surface water conditions which are closer to the biological optimum of a certain species lead to an increased average test size. This explains why in most cases a larger average test size of a species covaries with higher mass accumulation rates, as also the production of tests increases when conditions are favorable (Naidu, 1995). In addition, reproductive cycles, which may be related to lunar cyclicity, do have a profound effect on the shape of SFDs of living populations and those collected by sediment traps (Bijma et al., 1994).

(2) Differences in weight (as a function of size) and presence/absence of spines mainly controls the sinking speed of foraminifera (Takahashi and Bé, 1984; Bijma et al., 1994). Large, adult and non-spinose species therefore reach the sea floor faster than smaller spinose ones. However, juveniles and adult specimens that die without undergoing gametogenesis do not drop their spines, resulting in a lower settling velocity than specimens that underwent gametogenesis (J. Bijma, pers. commun., 1998). Consequently, the residence time of a certain species in the water column increases with decreasing test size. Berger (1971) noted that: “Size distributions suggest that most of the foraminiferal production becomes

Plate II

All specimens from the Last Glacial Maximum sample. Scale bar = 100 μm.

1–2. Adult *Neogloboquadrina dutertrei* from size fraction 355–400 μm.
1. Umbilical view.
2. Spiral view.
3–4. Small adult *Neogloboquadrina dutertrei* from size fraction 180–212 μm.
3. Umbilical view.
4. Spiral view.
5–6. Adult *Neogloboquadrina pachyderma* from size fraction 180–212 μm.
5. Umbilical view.
6. Spiral view.

Size frequency distributions of the dextral *Neogloboquadrina*-complex (*N.dutertrei* and *N.pachyderma*)

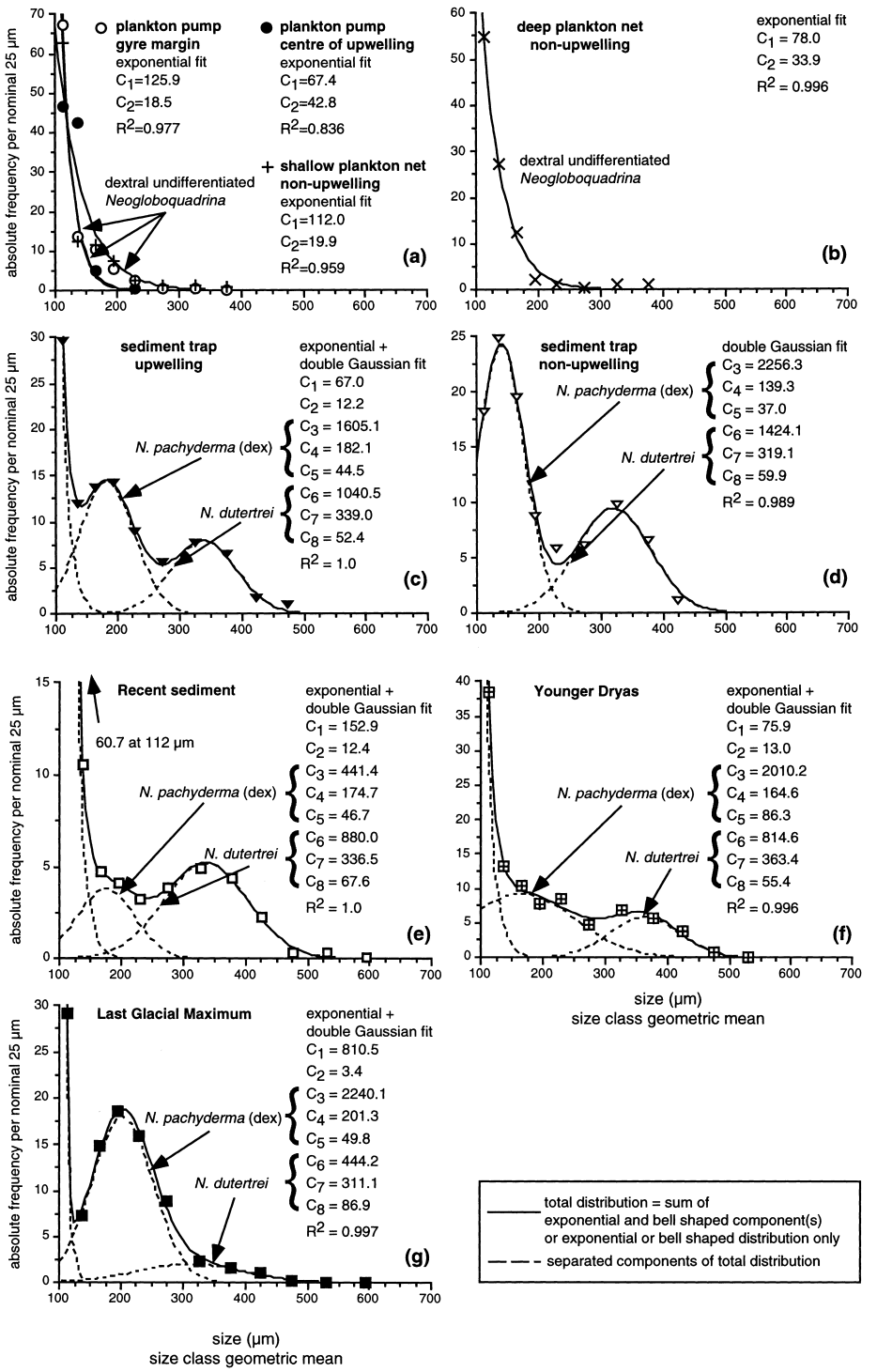

food for predators and is not available for sedimentation". Because larger specimens (species) sink faster from the productive zone than the smaller ones, the likelihood that small specimens become food or are affected by dissolution also increases with decreasing test size. This might explain the consistent over-representation of relatively small specimens in surface water compared to sediment trap and sediment distributions. Consequently, larger specimens and also larger species have greater fossilization potential than smaller ones. In addition, specimens which die without gametogenesis are filled with cytoplasm, which is probably assimilated by bacteria producing a micro-environment that favors dissolution. Therefore, it may be anticipated that small sized species and specimens that did not undergo gametogenesis are consistently underrepresented in the fossil record.

(3) Although our samples did not show any signs of carbonate dissolution, it may selectively remove smaller sized specimens and thus affect their SFD.

(4) Finally, winnowing may selectively remove the finer specimens after the foraminifera settled on the sea floor.

5.3. Selection of sieves

When comparing the work of different authors who used sieves of unequal mesh size, it is useful to consider water column (concentration) and sediment trap/sediment (settling flux) samples separately. Most of the species in surface water have an exponential SFD. This exponential trend might be used to predict numbers of specimens in any part of the size spectrum. However, Bijma and Hemleben (1994) and our own data show that this exponential trend is not always present and SFDs may show a maximum in the coarser part of the size spectrum (coarser fractions) as a result of ontogenetic development of the population, obstructing a possible extrapolation of observations from one size fraction to the other.

Although the selection of the sieve mesh sizes for faunal analysis should be based on the specific research questions first, fractionation of the size spectrum is often necessary to separate larger from the smaller specimens, which are more difficult to identify. In size fractions larger than 150 μm most species have reached the adult stage of ontogeny and we recommend this mesh size for standard faunal analysis. In addition sieve mesh sizes of 125 and 250 μm have be used in order to obtain a statistically significant estimate of small and large species, respectively. Their relative abundance will otherwise be overwhelmed in case only a sieve mesh size of 125 μm is used (rare fraction effect). For example, adult *N. pachyderma* (sin) is almost exclusively present in fractions smaller than 150 μm in samples from the Arabian Sea upwelling areas (Ivanova et al., 1999).

5.4. Average test size

Previous studies on size variations in planktic foraminifera indicated that size variations form mappable geographic patterns. Also, tropical species are larger in warm than in cooler waters and decrease in size with increasing latitude, while polar species behave in an opposite manner (Stone, 1956; Kennett, 1968; Bé et al., 1973; Hecht, 1974, 1976). Hecht (1976) studied size variations of some Recent planktic foraminifer species in the >250 μm fraction of 56 core-tops from the North Atlantic, and concluded that species reach their maximum average test size (= arithmetic test size of specimens >250 μm) in regions of 'optimum' temperatures and salinities. Naidu and Malmgren (1995) used an average test size cross sectional area as an index for upwelling intensity in the Arabian Sea. They concluded that shell-mass accumulation rates of *G. bulloides*,

Fig. 10. Size frequency distributions of the dextral *Neogloboquadrina* complex (*Neogloboquadrina dutertrei* and *Neogloboquadrina pachyderma* + P–D intergrades) in surface water (a) and in the deep water samples (b–d). The size frequency distribution in surface water and in the deep plankton net is exponential, whereas in the sediment trap and sediment samples (b–g) its distribution is bimodal. There, the smaller peak reflects adult *Neogloboquadrina pachyderma* and the larger adult specimens of *Neogloboquadrina dutertrei*. Separation of the Gaussian distributions is possible because the adult size of both species greatly differs. Note the much larger contribution of dextral *N. pachyderma* in the Last Glacial Maximum sample (g), compared to the Younger Dryas and Recent sediment (e–f). Coefficients C_1 to C_8 are those of Eq. 3, C_4 and C_7 represent the modal size of the smaller and larger population, respectively.

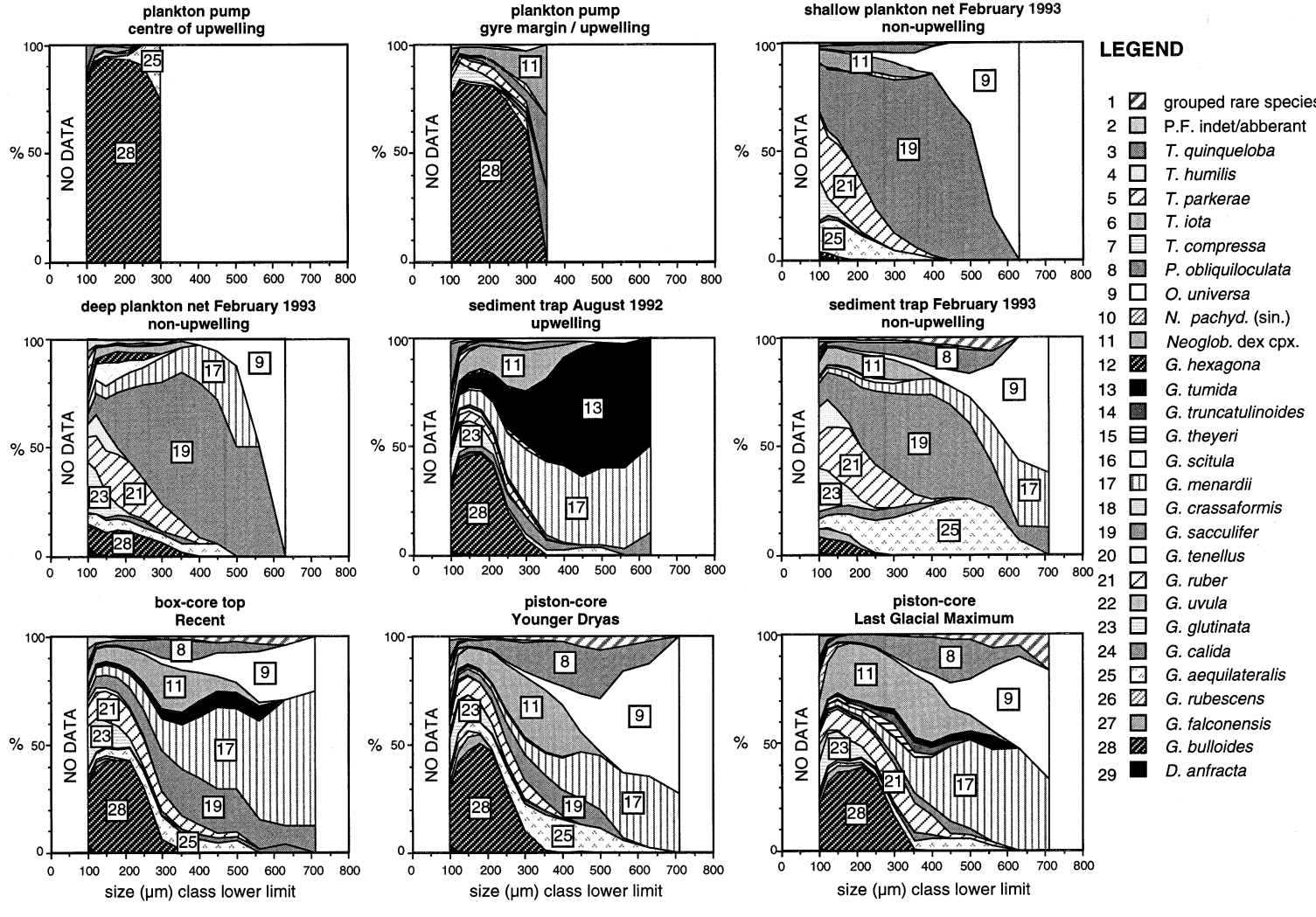

Fig. 11. Cumulative relative abundance of species across the size spectrum in surface water (top row), deep water (middle row) and sediment (base row). Note the effect of the sieve mesh size on the faunal composition. The composition of the total faunal assemblage for any sieve-mesh size can be read off on the vertical axis, using a sieve of the size given on the horizontal axis. Note large change in species composition between the upwelling and non-upwelling trap samples.

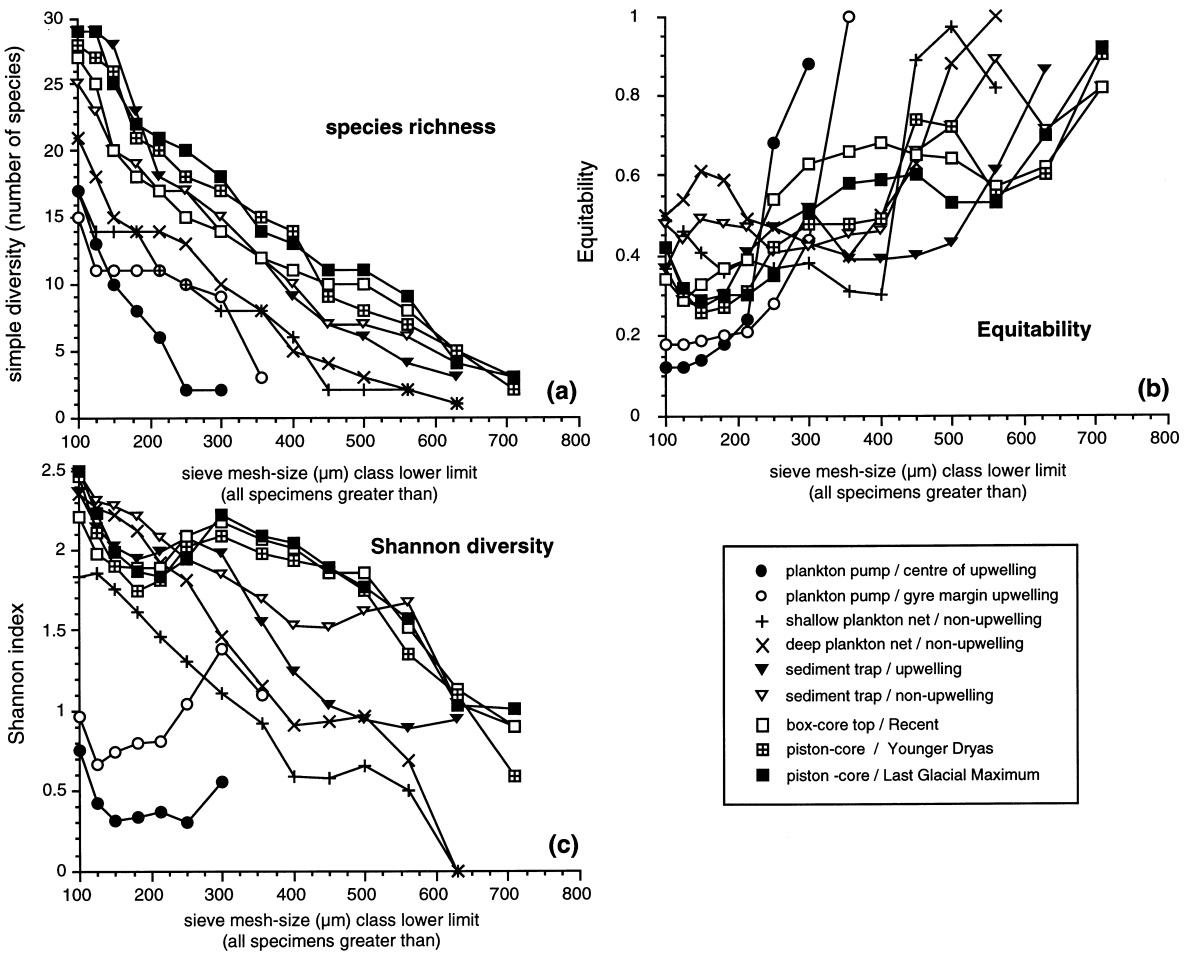

Fig. 12. Plot showing the effect of sieve mesh size on species richness (a), Shannon diversity (b) and equitability (c). At any sieve mesh size the values regard the total fauna larger than that size. Note the local minimum in the Shannon diversity in the 'upwelling' and sediment samples between 150 and 250 µm caused by dominant *G. bulloides*.

G. ruber, N. dutertrei and *G. glutinata*, are linearly proportional to their mean size, indicating that both mean size and productivity of individual species are related to upwelling intensity in the Arabian Sea. Most of the authors mentioned above studied relatively coarse size fractions, i.e. >150 µm (Naidu and Malmgren, 1995); and >250 µm (Hecht, 1976) and the observed variability in the average test size parameter is thus mainly the result of changes in the Gaussian distribution, reflecting larger specimens which reached the adult/terminal stage of ontogeny. In this part of the size spectrum, most of the specimens have undergone gametogenesis as is for example shown by Bijma and Hemleben (1994) for *G. sacculifer*. However, the calculation of an average test size strongly depends on the sieve which was used in the laboratory, and the results of different authors who used unequal mesh sizes can therefore not be compared. Generally, larger test sizes were measured in regions where conditions are closer to the apparent biological optimum of the species or, in case of living populations, it may be controlled by lunar or semi-lunar reproductive cycles (Bijma et al., 1990, 1994; Bijma and Hemleben, 1994). We have used one or two Gaussian distributions to analyze the distribution of adult specimens. In our examples, the average test size of these specimens is therefore similar to the modal value found at the center of the

Table 2
Percentage and cumulative percentage of total fauna per fraction. All foraminifera larger than 100 μm equal 100%

Size fraction	Surface water						Deep water						Sediment					
	plankton pump/ centre of upwelling		plankton pump/ gyre margin		shallow plankton net/ non-upwelling		deep plankton net/ non-upwelling		sediment trap/ upwelling		sediment trap/ non-upwelling		box-core top/ Recent		piston-core/ Younger Dryas		piston-core Last Glacial Maximum	
	%	cum. %	%	cum. %	%	cum. %	%	cum. %	%	cum. %	%	cum. %	%	cum. %	%	cum. %	%	cum. %
100–125	73.0	100.0	58.7	100.0	68.3	100.0	58.9	100.0	47.9	100.0	28.6	100.0	56.8	100.0	55.4	100.0	48.9	100.0
125–150	14.4	27.0	21.2	41.3	7.7	31.7	16.3	41.1	11.1	52.1	18.4	71.4	8.1	43.2	12.3	44.6	13.8	51.1
150–180	7.0	12.6	10.0	20.2	9.3	24.0	11.0	24.7	9.9	41.0	12.7	53.0	7.5	35.1	10.5	32.3	12.4	37.3
180–212	3.9	5.6	6.6	10.2	5.3	14.8	4.0	13.8	10.0	31.0	10.9	40.2	7.4	27.6	9.1	21.8	8.0	24.9
212–250	1.2	1.7	2.8	3.6	3.2	9.4	2.8	9.8	9.9	21.0	6.8	29.4	7.9	20.2	6.2	12.6	7.9	16.9
250–300	0.4	0.4	0.5	0.9	2.1	6.2	2.5	7.0	3.1	11.1	4.5	22.6	6.2	12.3	2.6	6.4	5.1	9.0
300–355	0.1	0.1	0.3	0.3	1.7	4.1	2.1	4.5	2.9	8.0	6.7	18.1	2.5	6.1	1.7	3.8	2.3	3.9
355–400			0.0	0.0	0.8	2.4	1.2	2.4	1.4	5.1	3.8	11.4	1.3	3.7	0.9	2.0	0.8	1.7
400–450					0.9	1.6	0.6	1.2	1.1	3.7	2.9	7.6	1.1	2.4	0.6	1.1	0.5	0.9
450–500					0.2	0.7	0.3	0.6	0.7	2.6	1.5	4.7	0.2	1.3	0.1	0.5	0.1	0.3
500–560					0.3	0.5	0.2	0.3	1.2	1.9	2.0	3.2	0.6	1.1	0.2	0.4	0.1	0.2
560–630					0.1	0.2	0.0	0.1	0.5	0.7	0.7	1.2	0.3	0.5	0.1	0.2	0.0	0.1
630–710					0.1	0.1	0.0	0.0	0.2	0.2	0.3	0.5	0.1	0.2	0.1	0.1	0.0	0.0
>710										0.1	0.1	0.1	0.1	0.1	0.0	0.0	0.0	0.0

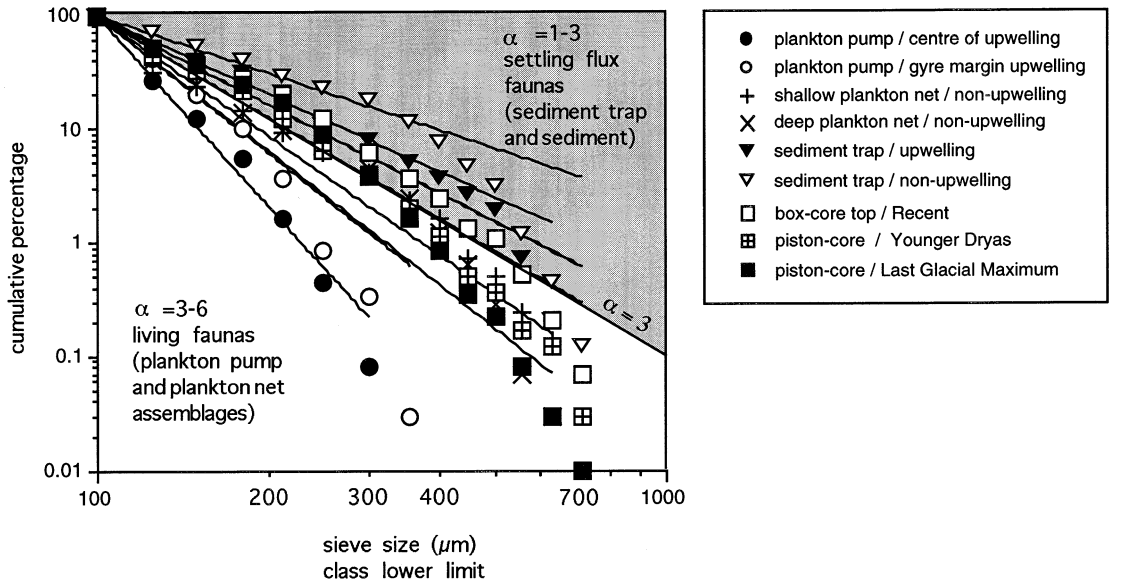

Fig. 13. Graph showing cumulative percentage of the total fauna larger than 100 μm against size. The total fauna as a function of size can be described using Eq. 7, in which values of α between 3 and 6 are related to 'water' samples (plankton pump and plankton net), whereas α values between 1 and 3 are related to 'flux' samples (sediment trap and sediment samples).

Gaussian distribution. The modal test size obtained from the Gaussian distribution does not necessarily reflect the average test size as obtained by measuring the foraminiferal test, which may include the pre-adult ones too. A modal test size of adult specimens obtained using the 'Gaussian method' will probably be closer to biological optimum size of the species.

6. Conclusions

Living populations of species (>100 μm), viz. in the photic zone, mostly show an exponential size frequency distribution (SFD), with highest numbers in the smallest part of the size spectrum. Samples from the deeper part of the ocean, plankton nets, sediment traps and core samples, recorded an integrated settling flux over longer time spans from hours to hundreds of years. The SFDs of species in those samples may consist of: (a) an exponential distribution of relatively small immature specimens; (b) a Gaussian shaped distribution reflecting larger specimens which reached the adult/terminal stage of ontogeny; or (c) a combination of both. The distributions are separated using a best fit approach, providing quantitative information on modal size of adult specimens, as well as their distribution width over the size spectrum.

The SFD of species is controlled by several factors: time and duration of sample collection and differences in settling speed of smaller and larger tests. Dissolution and winnowing may selectively remove the smaller specimens. The consistent underrepresentation of smaller specimens in sediment and sediment trap assemblages, compared to living faunas as collected by plankton pump and net, is explained by the fact that larger specimens descend faster to the sea floor than smaller ones, reducing the likelihood that they are destroyed by predation and dissolution in the water column.

Because the SFD of a certain species is variable, the average size of specimens varies from sample to sample. Calculating a simple arithmetic average test size from all tests or obtaining an average test size from the mode of a fitted Gaussian distribution may yield contradictory results. The latter may prove more useful in paleoceanographic studies, as it will probably be closer to the biological optimum size of the species.

The total fauna in a sample is the sum of individual species distributions. Consequently, the fauna as a function of sieve mesh size depends on (a) the species composition, (b) the absolute abundance of individual species and (c) their size frequency distribution, which is determined by the ontogenetic stage and environmental conditions present at time of sample collection.

In the water column approximately 60% of the fauna (>100 μm) is present in the 100–125 μm fraction and 1–6% is larger than 250 μm. In samples representing a settling flux (sediment trap and sediment samples) 29–57% of the fauna is present in the 100–125 μm fraction, while 6–23% is larger than 250 μm.

Dextral *N. pachyderma* and *N. dutertrei* often show a morphological gradation (P–D intergraded). The size frequency distribution of the *Neogloboquadrina* complex (= *N. dutertrei*, *N. pachyderma* and P–D intergrades) shows a bimodal pattern. Because the modal size of adult specimens of both species differs by 90 to 200 μm, the size frequency distributions of the individual species can be separated using a bimodal curve fitting technique.

In size fractions larger than 150 μm most species have reached the adult stage of ontogeny and we recommend this mesh size for standard faunal analysis. In addition sieve mesh sizes of 125 μm and 250 μm have to be used to obtain a reliable estimate of small and large species, respectively. Their relative abundance will otherwise be overwhelmed in case only a sieve mesh size of 125 μm is used (rare fraction effect). Finer fractions are increasingly dominated by small species and pre-adult specimens of larger species.

Acknowledgements

We acknowledge sponsoring by the Dutch Organization for Scientific Research (NWO). The Netherlands Indian Ocean Programme was funded and coordinated by the Netherlands Marine Research Foundation (SOZ) of the Netherlands Organization for Scientific Research (NWO). This is publication No. 980708. of the Netherlands Research School of Sedimentary Geology and No. 3257 of the Netherlands Institute for Sea Research (NIOZ). S. Kars is thanked for making the SEM pictures. We thank J. Bijma and an anonymous reviewer for helpful comments and reviewing the final version of this manuscript.

Appendix A

The relative abundance of species in surface waters. Species percentages are plotted for each individual size fraction against sieve class lower limit.

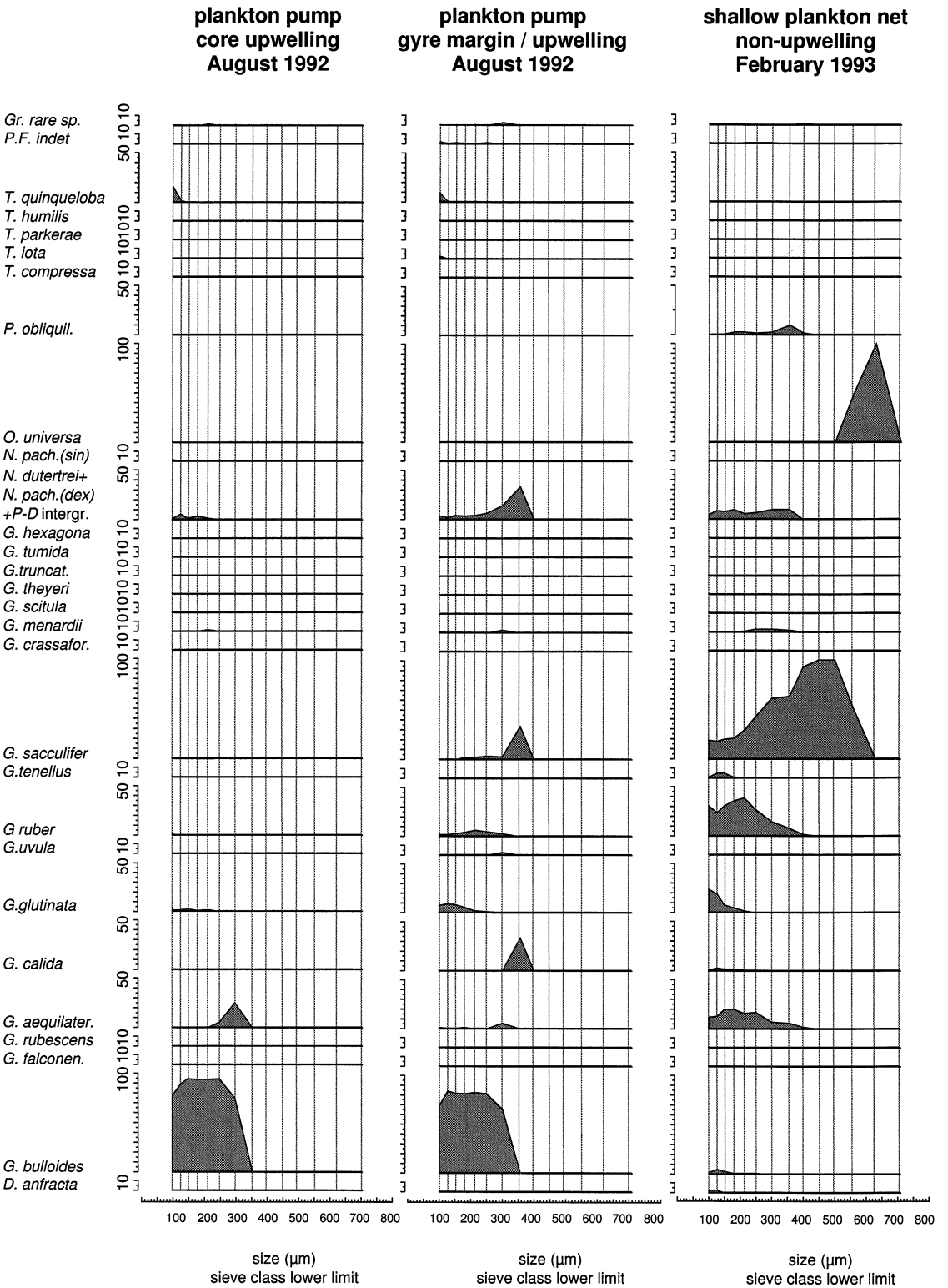

Appendix B

The relative abundance of species in deep plankton net and sediment trap samples. Species percentages are plotted for each individual size fraction against sieve class lower limit.

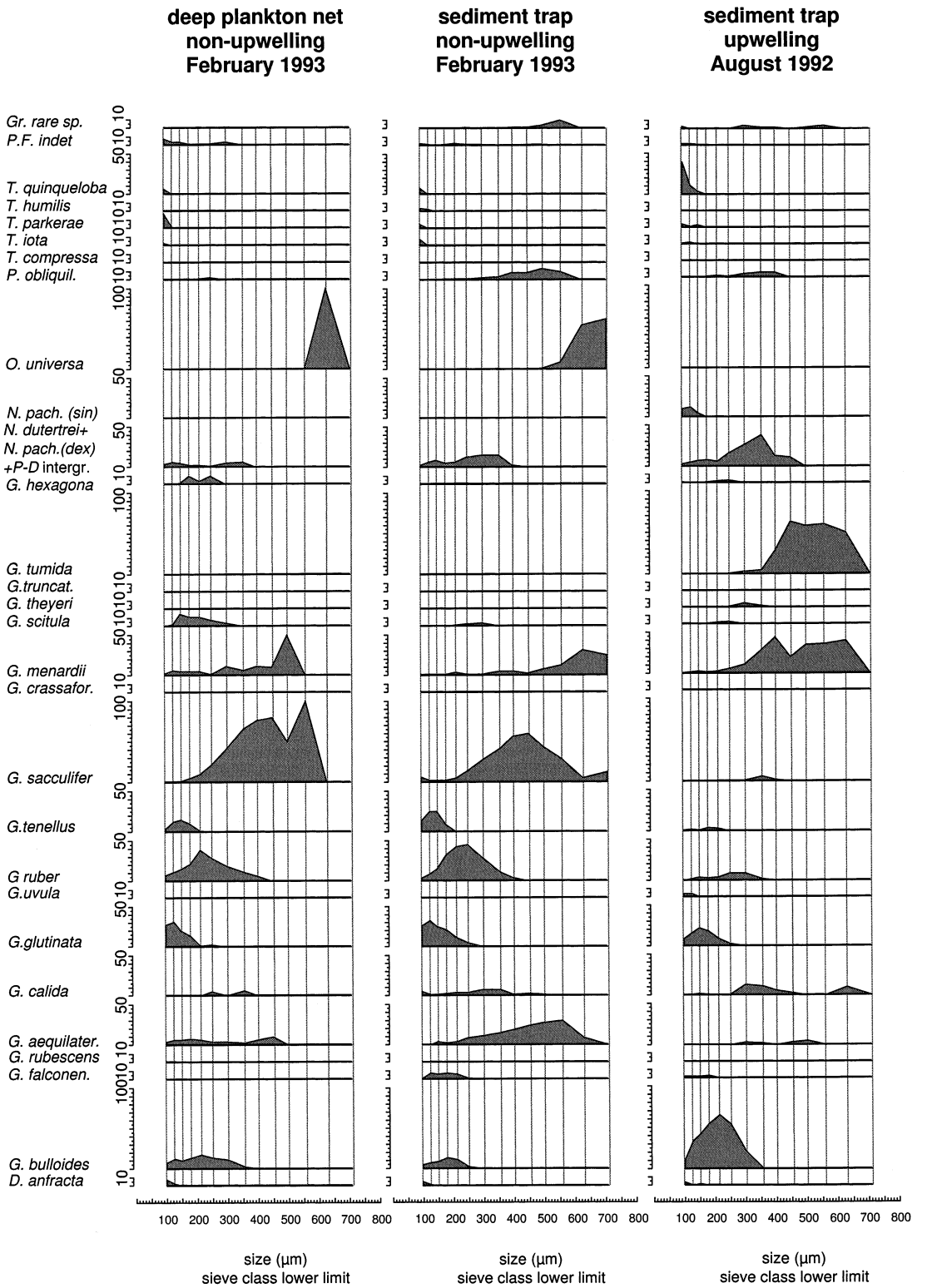

Appendix C

The relative abundance of species in sediment samples. Species percentages are plotted for each individual size fraction against sieve class lower limit.

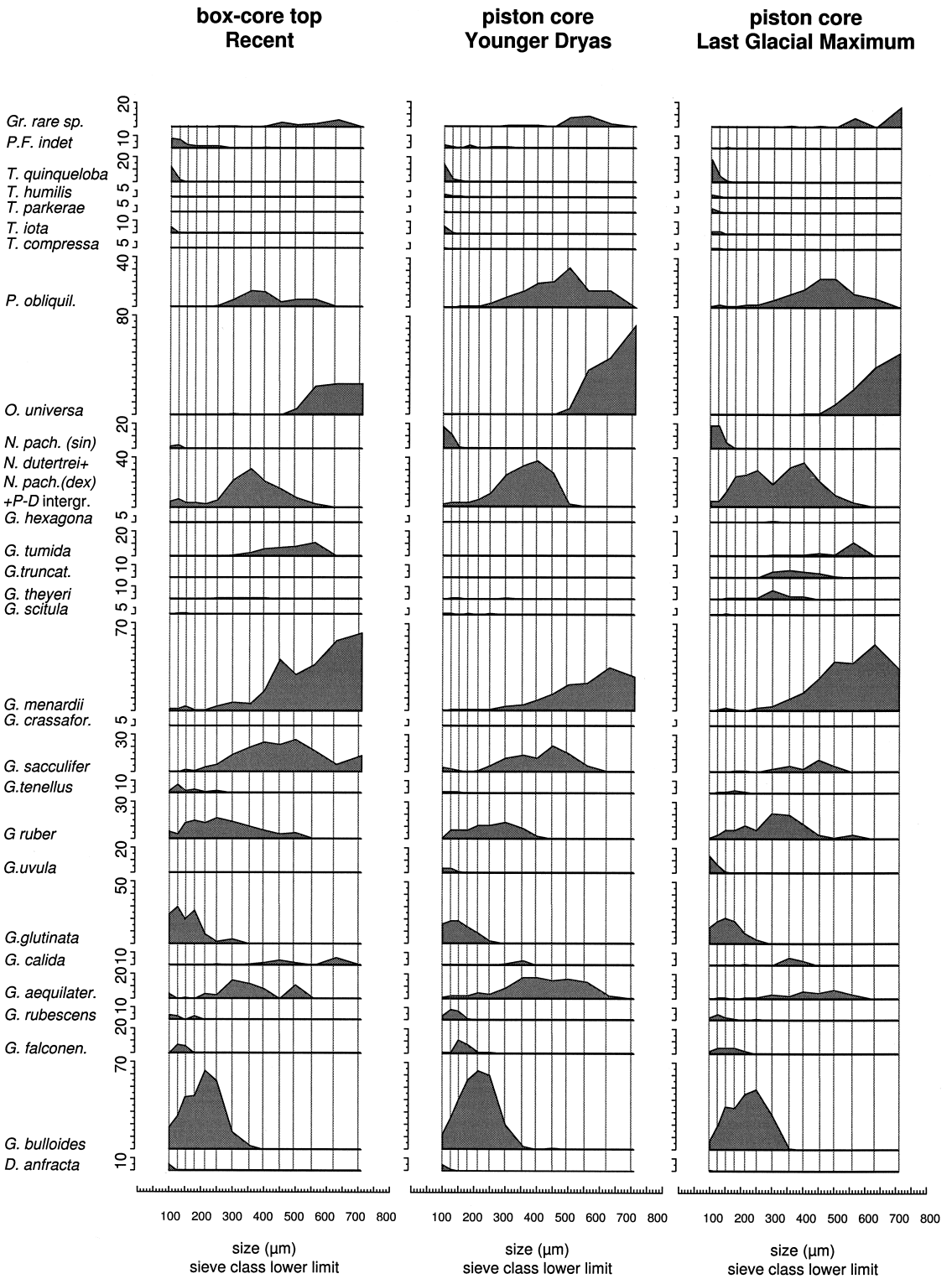

References

Anderson, D.M., Prell, W.L., 1993. A 300 kyr record of upwelling off Oman during the Late Quaternary: evidence of the Asian southwest monsoon. Paleoceanography 8 (2), 193–208.

Banse, K., 1987. Seasonality of phytoplankton chlorophyll in the central and northern Arabian Sea. Deep-Sea Res. 34, 713–723.

Bé, A.W.H., 1967. Foraminifera families: *Globigerinidae* and *Globorotaliidae*. In: Fiches d'Identification du Zooplankton, sheet 108. Conseil permanent international pour l'exploration de la mer, Charlottenlund, Denmark, pp. 1–3.

Bé, A.W.H., 1980. Gametogenic calcification in a spinose planktonic foraminifer, *Globigerinoides sacculifer* (Brady). Mar. Micropaleontol. 5, 283–310.

Bé, A.W.H., Hutson, W.H., 1977. Ecology of planktonic foraminifera and biogeographic patterns of life and fossil assemblages in the Indian Ocean. Micropaleontology 23, 369–414.

Bé, A.W.H., Harrison, S.M., Lott, L., 1973. *Orbulina universa* d'Orbigny in the Indian Ocean. Micropaleontology 19, 150–192.

Berger, W.H., 1969. Ecologic patterns of living planktonic foraminifera. Deep-Sea Res. 169, 1–24.

Berger, W.H., 1971. Sedimentation of planktonic foraminifera. Mar. Geol. 11, 325–358.

Bijma, J., Hemleben, C., 1994. Population dynamics of the planktic foraminifer *Globigerinoides sacculifer* (Brady) from the central Red Sea. Deep-Sea Res. I 41, 485–510.

Bijma, J., Erez, J., Hemleben, C., 1990. Lunar and semi-lunar reproductive cycles in some spinose planktonic foraminifers. J. Foraminiferal Res. 20, 117–127.

Bijma, J., Hemleben, C., Wellnitz, K., 1994. Lunar-influenced carbonate flux of the planktic foraminifer *Globigerinoides sacculifer* (Brady) from the central Red Sea. Deep-Sea Res. I 41, 511–530.

Blanco, J.M., Echevarria, F., Garcia, C.M., 1994. Dealing with size spectra: some conceptual and mathematical problems. Sci. Mar. 58 (12), 17–29.

Bruce, J.G., 1979. Eddies off the Somali coast during the southwest monsoon. J. Geophys. Res. 84, 7742–7748.

Bruce, J.G., Quadfasel, D.R., Swallow, J.C., 1980. Somali eddy formation during the commencement of the southwest monsoon, 1978. J. Geophys. Res. 85, 6654–6660.

Brummer, G.J.A., 1995. Plankton pump and multinet. In: Van Hinte, J.E., Van Weering, Tj.C.E., Troelstra, S.R. (Eds.), Tracing a Seasonal Upwelling. Report on two cruises of RV *Tyro* to the NW Indian Ocean in 1992 and 1993. National Museum of Natural History, Leiden, pp. 31–45.

Brummer, G.J.A., Kroon, D., 1988. Planktonic Foraminifers as Tracers of Ocean-Climate History. Free Univ. Press, Amsterdam, 346 pp.

Buzas, M.A., Gibson, T.G., 1969. Species diversity: benthonic Foraminifera in Western North Atlantic. Science 163, 72–75.

Caron, D.A., Bé, A.W.H., Anderson, O.R., 1981. Effects of variations in light intensity on life processes of the planktonic foraminifer *Globigerinoides sacculifer* in laboratory culture. J. Mar. Biol. Assoc. U.K. 62, 1981.

Caulet, J.P., Vénec-Peyré, M., Vergnaud-Grazzini, C., Nigrini, C., 1992. Variation of South Somalian upwelling during the last 160 ka: radiolarian and foraminifera records in core MD85674. In: Summerhays, C.P., Prell, W.L., Emeis, K.C. (Eds.), Upwelling Systems: Evolution since the Early Miocene. Geol. Soc. Spec. Publ. 64, 379–389.

Clemens, S., Prell, W.L., Murray, D., Shimmield, G., Weedon, G., 1991. Forcing mechanisms of the Indian Ocean monsoon. Nature 353, 720–725.

CLIMAP, 1981. Seasonal reconstruction of the earth's surface at the last glacial maximum. Geol. Soc. Am. Map Chart Ser. MC-36.

CLIMAP, 1984. The last interglacial. Quat. Res. 21, 123–224.

Conan, S.M.-H., Brummer, G.J.A., 1999. Fluxes of planktic foraminifera in response to monsoonal upwelling on the Somalia Basin margin. Deep-Sea Res. (in press).

Cullen, J.L., Prell, W.L., 1984. Planktic foraminifera of the northern Indian ocean: distribution and preservation in surface sediments. Mar. Micropaleontol. 9, 1–52.

Curry, W.B., Matthews, R.K., 1981. Paleo-oceanographic utility of oxygen isotopic measurements on planktic foraminifera: Indian Ocean core-top evidence. Palaeogeogr., Palaeoclimatol., Palaeoecol. 33, 173–191.

Curry, W.B., Ostermann, D.R., Gupta, M.V.S., Ittekkot, V., 1992. Foraminiferal production and monsoonal upwelling in the Arabian Sea: evidence from sediment traps. In: Summerhays, C.P., Prell, W.L., Emeis, K.C. (Eds.), Upwelling Systems: Evolution since the Early Miocene. Geol. Soc. Spec. Publ. 64, 93–106.

Erez, J., Almogi-Labin, A., Avraham, S., 1991. On the life history of planktonic foraminifera: lunar reproduction cycle in *Globigerinoides sacculifer* (Brady). Paleoceanography 6 (3), 295–306.

Fisher, J., Schott, F., Schott, L.S., 1996. Currents and transports of the Great Whirl–Socotra Gyre system during the summer monsoon, August 1993. J. Geophys. Res. 101, 3573–3587.

Ganssen, G., Kroon, D., 1991. Evidence for Red Sea surface circulation from oxygen isotopes of modern surface waters and planktonic foraminiferal tests. Paleoceanography 6, 73–82.

Giraudeau, J., Rogers, J., 1994. Phytoplankton biomass and sea-surface temperature estimates from sea-bed distribution of nannofossils and planktic foraminifera in the Benguela upwelling system. Micropaleontology 40, 275–285.

Guptha, M.V.S., Mohan, R., Muralinath, A.S., 1994. Living planktonic foraminifera during the late summer monsoon period in the Arabian Sea. Mar. Geol. 120, 365–371.

Hecht, A.D., 1974. Intraspecific variation in Recent populations of *Globigerinoides ruber* and *Globigerinoides trilobus* and their application to paleoenvironmental analysis. J. Paleontol. 48, 1217–1234.

Hecht, A.D., 1976. An ecologic model for test size variation in Recent planktonic foraminifera: applications to the fossil record. J. Foraminiferal Res. 6, 295–311.

Hemleben, C., Spindler, M., Anderson, O.R., 1989. Modern Planktonic Foraminifera. Springer, 363 pp.

Hilbrecht, H., 1997. Morphologic gradation and ecology in *Neogloboquadrina pachyderma* and *Neogloboquadrina dutertrei* (planktic foraminifera) from core top sediments. Mar. Micropaleontol. 31, 31–43.

Imbrie, J., Kipp, N.G., 1971. A new micropaleontological method for quantitative paleoclimatology: Application to a late Pleistocene Caribbean core. In: Turekian, K.K. (Ed.), The Late Cenozoic Ages. Yale Univ. Press, New Haven, CT, pp. 71–181.

Ivanova, E.M., Conan, S.M.-H., Peeters, F.J.C., Troelstra, S.R., 1999. *Neogloboquadrina pachyderma* (sin) in the Oman and Somalia upwelling areas. Mar. Micropaleontol. (in press).

Kennett, J.P., 1968. Latitudinal variations in *Globigerina pachyderma* in surface sediments of the southwest Pacific Ocean. Micropaleontology 14, 305–318.

Kipp, N.G., 1976. New transfer function for estimating past sea surface conditions from sea bed distribution of planktic foraminiferal assemblages in the North Atlantic. In: Cline, R.M., Hays, J.D. (Eds.), Investigations of Southern Ocean Paleoceanography and Paleoclimatology. Mem. Geol. Soc. Am. 145, 3–42.

Kroon, D., Darling, K., 1995. Size and upwelling control of the stable isotope composition of *Neogloboquadrina dutertrei* (D' Orbigny), *Globigerinoides ruber* (D'Orbigny) and *Globigerina bulloides* (D'Orbigny): examples from the Panama Basin and Arabian Sea. J. Foraminiferal Res. 25, 39–52.

Kroon, D., Ganssen, G., 1989. Northern Indian Ocean upwelling cells and the stable isotope composition of living planktonic foraminifers. Deep-Sea Res. 36, 1219–1236.

Lipps, J.H., Berger, W.H., Buzas, M.A., Douglas, R.G., Ross, C.A., 1979. Foraminiferal ecology and paleoecology. SEPM Short Course 6.

Naidu, P.D., 1995. High-resolution studies of Asian Quaternary monsoon climate and carbonate records from the Equatorial Indian Ocean. Ph.D. Thesis, Göteborg Univ., Göteborg.

Naidu, P.D., Malmgren, B.A., 1995. Monsoon upwelling effects on test size of some planktic foraminiferal species from the Oman margin, Arabian sea. Paleoceanography 10, 117–122.

Naidu, P.D., Malmgren, B.A., 1996a. Relationship between Late Quaternary upwelling history and coiling properties of *N. pachyderma* and *G. bulloides* in the Arabian Sea. J. Foraminiferal Res. 26, 64–70.

Naidu, P.D., Malmgren, B.A., 1996b. A high-resolution record of late Quaternary upwelling along the Oman Margin, Arabian Sea based on planktonic foraminifera. Paleoceanography 11, 129–140.

Ottens, J.J., 1992. Planktic foraminifera as indicators of ocean environments in the Northeast Atlantic. Thesis, Free Univ. Press, Amsterdam, 189 pp.

Pflaumann, U., Duprat, J., Pujol, C., Labeyrie, L.D., 1996. SIMMAX: A modern analog technique to deduce Atlantic sea surface temperatures from planktic foraminifera in deep-sea sediments. Paleoceanography 11, 15–35.

Pickard, G.L., 1979. Descriptive Physical Oceanography. Pergamon, 233 pp.

Prell, W.L., Curry, W.B., 1981. Faunal and isotopic indices of monsoonal upwelling: western Arabian Sea. Oceanol. Acta 4, 91–98.

Prell, W.L., Kutzbach, J.E., 1992. Sensitivity of the Indian monsoon to forcing parameters and implications for its evolution. Nature 360, 647–652.

Prell, W.L., Van Campo, E., 1986. Coherent response of Arabian Sea upwelling and pollen transport to late Quaternary monsoonal winds. Nature 323, 526–528.

Prell, W.L., Murray, D.W., Clemens, S.C., Anderson, D.M., 1992. Evolution and variability of the Indian Ocean summer monsoon: Evidence from the Western Arabian Sea Drilling Program. Synthesis of results from scientific drilling in the Indian Ocean. Geophys. Monogr. 70.

Reichart, G.J., 1997. Late Quaternary variability of the Arabian Sea monsoon and oxygen minimum zone. Univ. Utrecht, Utrecht, 173 pp.

Schiebel, R., Bijma, J., Hemleben, C., 1997. Population dynamics of the planktic foraminifer *Globigerina bulloides* from the eastern North Atlantic. Deep-Sea Res. 44, 1701–1713.

Schott, F., Swallow, J.C., Fieux, M., 1990. The Somali current at the equator: annual cycle of currents and transports in the upper 1000 m and connection to neighbouring latitudes. Deep-Sea Res. 37 (12), 1825–1848.

SCOR, 1990. Core measurements protocols. Reports of the Core Measurement Working Groups. JGOFS Rep. 6, SCOR, Dalhousie Univ., Halifax, pp. 40.

Signes, M., Bijma, J., Hemleben, C., Ott, R., 1993. A model for planktic foraminiferal shell growth. Paleobiology 19 (1), 71–91.

Steens, T.N.F., Ganssen, G., Kroon, D., 1992. Oxygen and carbon isotopes in planktic foraminifera as indicators of upwelling intensity and upwelling-induced high productivity in sediments from the north-western Arabian Sea. In: Summerhays, C.P., Prell, W.L., Emeis, K.C. (Eds.), Upwelling Systems: Evolution since the Early Miocene. Geol. Soc. Spec. Publ. 64, 107–119.

Stone, S.W., 1956. Some ecologic data relating to pelagic foraminifera. Micropaleontology 2, 361–370.

Swallow, J.C., Bruce, J.G., 1966. Current measurements off the Somali coast during the southwest monsoon of 1964. Deep-Sea Res. 13, 861–888.

Takahashi, K., Bé, A.D., 1984. Planktonic foraminifera: factors controlling sinking speeds. Deep-Sea Res. 31, 1477–1500.

Van Hinte, J.E., Van Weering, Tj.C.E., Troelstra, S.R., 1995. Tracing a seasonal upwelling. Report on two cruises of RV *Tyro* to the NW Indian Ocean in 1992 and 1993. National Museum of Natural History, Leiden.

Vella, P., 1974. Coiling ratios of *Neogloboquadrina pachyderma* (Ehrenberg): variations in different size fractions. Geol. Soc. Am. Bull. 85, 1421–1424.

Vénec-Peyré, M.-T., Caulet, J.P., Vergnaud Grazzini, C., 1995. Paleohydrographic changes in the Somali Basin (5ºN upwelling and equatorial areas) during the last 160 kyr, based on correspondence analysis of foraminiferal and radiolarian assemblages. Paleoceanography 10, 473–491.

Vergnaud-Grazzini, C., Vénec-Peyré, M.T., Caulet, J.P., Lerasle, N., 1995. Fertility tracers and monsoon forcing at an equatorial site of the Somali basin (Northwest Indian ocean). Mar. Micropaleontol. 26, 137–152.

Zhang, J., 1985. Living planktonic foraminifera from the eastern Arabian Sea. Deep-Sea Res. 32 (7), 789–798.